SilkBridge™: A novel biomimetic and biocompatible silk-based nerve conduit

SilkBridge™: a novel biomimetic and biocompatible silk-based nerve conduit

A. Alessandrino[1], F. Fregnan[2,3], M. Biagiotti[1], L. Muratori[2,3], G.A. Bassani[1], G. Ronchi[2,3], V. Vincoli[1], P. Pierimarchi[4], S. Geuna[2,3], G. Freddi[1]*

[1]Silk Biomaterials Srl, 22074 Lomazzo (Co), Italy; [2]Department of Clinical and Biological Sciences, University of Torino, 10124 Torino, Italy; [3]Neuroscience Institute Cavalieri Ottolenghi, University of Torino, 10124 Torino, Italy; [4]Institute of Translational Pharmacology, National Research Council, 00083 Rome, Italy.

*Corresponding author: giuliano@silkbiomaterials.com

Running title: SilkBridge™ nerve conduit

Abstract

Silk fibroin (*Bombyx mori*) was used to manufacture a nerve conduit (SilkBridge™) characterized by a novel 3D architecture. The wall of the conduit consists of two electrospun layers (inner and outer) and one textile layer (middle), perfectly integrated at the structural and functional level. The manufacturing technology conferred high compression strength on the device, thus meeting clinical requirements for physiological and pathological compressive stresses. *In vitro* cell interaction studies were performed through direct contact assays with SilkBridge™ using the glial RT4-D6P2T cells, a schwannoma cell line, and Mouse Motor Neuron NSC-34 cell line. Results revealed that the material is capable to sustain cell proliferation, that the glial RT4-D6P2T cells increased their density and organized themselves in a glial-like morphology, and that NSC-34 motor neurons exhibited a greater neuritic length with respect to the control substrate. *In vivo* pilot assays were performed on adult females Wistar rats. A 10 mm long gap in the median nerve was repaired with 12 mm SilkBridge™. At two weeks post-operative several cell types colonized the lumen. Cells and blood vessels were also visible between the different layers of the conduit wall. Moreover, the presence of regenerated myelinated fibers with a thin myelin sheath at proximal level was observed. Taken together, all these results demonstrated that SilkBridge™ has an optimized balance of biomechanical and biological properties, being able to sustain a perfect cellular colonization of the conduit and the progressive growth of the regenerating nerve fibers.

Keywords: silk fibroin; nerve conduit; morphological structure; compression strength; *in vitro* biocompatibility; *in vivo* pilot test

1. INTRODUCTION

The incidence of traumatic peripheral nerve injuries is reported to affect annually hundreds of thousand individuals [1-3]. Motor and sensor disabilities, as well as neuropathic pain are caused by nerve injuries, which not only impair patient's quality of life but also significantly contribute to the annual health care costs. Most traumatic nerve injuries are caused by mechanical stresses (compression, traction, transection), which may involve upper extremity, more frequently radial, ulnar and median nerves [4,5], or lower extremity, more frequently sciatic and peroneal nerves [1]. Depending on the severity of the lesion (myelin, axon, or nerve disruption), self-repair may occur through axonal regeneration or surgical intervention may be required. Endoneurial and perineurial disruption, fascicular structure damage, axonal misdirection, formation of fibrosis or neuroma usually require surgical management of the lesions, which becomes mandatory whenever nerve continuity is interrupted and reinnervation through the physiological nerve regeneration capacity could not take place [1].

Surgical repair of nerve transection injuries can be accomplished by a variety of techniques, including end-to-end suturing, autologous nerve grafting, acellular and cellular allografts, nerve conduits. The type of surgical approach is dependent on several factors such as the length of the nerve gap, patient characteristics, injury type and location, nerve diameter, availability of proximal stump. Habre et al. [2] proposed an algorithm of treatment for open and closed nerve injuries where classes of gap length from <1 cm up to >10 cm are considered, and the best repairing options are indicated. For nerve gaps less than 1 cm, tension-free end-to-end suturing with correct fascicular alignment is the gold standard for surgical intervention. A wider range of techniques, such as autografts, cellular and acellular grafts, and nerve conduits can be used to treat monofascicular nerve gaps ranging from 1 to 5 cm, when proximal stump is available. Larger nerves with multiple fascicles (diameter >7 mm) are preferably treated with cable nerve grafts using group fascicular repair technique (autografts or allografts). For gaps greater than 5 cm, synthetic nerve conduits may fail, while autografts and acellular allografts may exhibit decreased efficiency due to the increased distance of regenerating axons. In this case, nerve transfers and vascularized nerve grafts (VNGs) appear more indicated approaches [1,2,6].

Nerve conduits for peripheral nerve regeneration are "off the shelf" available options for repairing nerve gaps of ≤3 cm, with nerve diameter in the 2-6 mm range [1-3]. They are tubular devices with luminal diameter large enough to host the proximal and distal ends of the severed nerve, which are held in place by suture stitches. Nerve conduits represent a feasible surgical alternative to autografts, especially when donor sites are limited in availability or drawbacks like mismatch between donor and recipient sites, the possibility of functional loss, or formation of neuroma at the donor site must be avoided. Synthetic non-resorbable polymers (silicone, polyethylene glycol), synthetic resorbable

polymers (polyglycolic acid – PGA; polycaprolactone - PCL), and biopolymers (chitosan, alginate, keratin, silk fibroin, collagen and other extracellular matrix components) are used to manufacture nerve conduits, some of which are FDA approved.

Advantages and drawbacks of different polymer materials have been reviewed by various authors [2,7]. Silicone-based conduits first demonstrated the possibility of using polymer grafts to bridge nerve gaps and allowed clarifying the mechanisms underlying nerve regeneration within the tubular structure. However, their permanent non-resorbable nature led to a variety of problems such as fibrotic encapsulation, chronic nerve compression, and requirement of surgical revision to remove the conduit material. Resorbable PGA conduits sometimes displayed too short degradation time, not enough for complete nerve regeneration. Moreover, they degrade into lactic acid, whose acidity may be harmful for the biological microenvironment of the site of implantation. The use of copolymers with PCL decreased the impact of this problem at the expenses of a greater rigidity and a more difficult handling of the device. Collagen conduits, thanks to the capability of interacting with surrounding tissues, can enhance regeneration rate of defected nerves. However, complications such as fibrosis, “hourglassing” of the fibrin cable, and nerve compression have been reported. Polymers of different origin and properties are often used in blend or to make different parts of the device in order to take advantage of their respective properties, including density, porosity, mechanical strength, biocompatibility, and degradation ability.

The nerve conduits usually take the form of a single hollow tube which provides passive mechanical support to axon regeneration. However, incorporation of intraluminal channels or microtubes, or insertion of filaments into the inner space are modifications that may allow achieving better outcomes in axonal regeneration because they mimic the 3D architecture of nerve fascicles [7]. Advantages of using luminal fillers are to increase surface area, to provide support for cell attachment, to direct axonal growth and elongation thus avoiding inappropriate axon dispersion and corresponding inaccurate target reinnervation.

Multiple fabrication techniques are used to realize different nerve conduits architectures, from electrospinning to freeze drying, injection molding, dip coating, phase separation, porogen leaching, etc. [6]. Electrospinning has gained high interest as it allows fabricating scaffolds with a structure similar to that of extracellular matrix, with adjustable mechanical strength, and with variable degree of porosity, which can be optimized to control permeability to nutrients and oxygen for cells and to avoid loss of neurotrophic factors secreted by Schwann cells at the distal stump. Rapid prototyping techniques are nowadays available to manufacture designs with more complex 3D geometry, more controlled and reproducible density and porosity, internal structures able to provide topographic cues to increase axon regenerating rate, thus avoiding or minimizing end-organ (e.g. muscle) atrophy.

Furthermore, new strategies to enhance the regeneration process are based on loading the scaffold with neurotrophic factors, Schwann cells and/or stem cells [3,9-11].

Silk fibroin (SF), a biodegradable and biocompatible natural polymer, has the potential to become the biomaterial of choice for the development of a range of medical applications [12-14]. The starting material can be easily purified and processed in different 2D/3D shapes with tunable mechanical properties and biodegradability. It is biocompatible, not immunogenic in humans and favors angiogenesis, a feature essential for tissue repair/regeneration. SF has been widely explored as a starting material for manufacturing conduits for peripheral nerve repair and regeneration [15]. Xue et al. [16] used the electrospinning technique to prepare a SF conduit of about 5 mm inner diameter, filled with 300 degummed SF filaments, for bridging a 30 mm long sciatic nerve gap in dogs. Twelve months after surgery, the results indicated that the SF-based scaffold achieved satisfactory regenerative outcomes, close to those achieved by autologous nerve grafts. Injection molding technique was used to manufacture a SF-based conduit filled with 20 degummed SF filaments to bridge a 10 mm long sciatic nerve defect in rats [17]. Dorsal Root Ganglia and Schwann cells were cultured *in vitro* and introduced into the conduit to create a tissue engineered nerve graft. Twelve weeks after nerve grafting authors noticed accelerated axonal growth and functional recovery, which was closer to that of the autologous nerve graft and better than that of the SF scaffold alone. As a biological strategy to enhance speed and quality of axon growth and to improve nerve regeneration and repair, neurotrophic/angiogenic factors [18], Schwann cells [19], stem cells [20] were incorporated into SF-based conduits, to establish a native-like microenvironment for nerve regeneration and to reduce the need of using nerve autografts.

Several studies have also explored the use of SF in combination with other natural or synthetic biocompatible and biodegradable polymers, with the aim of improving morphological, mechanical, and biological performance of the scaffold. Wang et al. [21] blended SF with poly(l-lactide-*co*-ε-caprolactone; P(LLA-CL)) and manufactured a nerve conduit by electrospinning to bridge 10 mm length nerve defects in rats. They found that SF/P(LLA-CL) nerve conduits enhanced peripheral nerve regeneration by improving angiogenesis, as shown by the significantly larger blood vessel area. In another study [22], SF was blended with collagen and a scaffold was prepared by injection molding. A set of SF/collagen conduits was loaded with Schwann cells and adipose-derived stem cells to obtain a tissue engineered nerve conduit. Conduits with and without cells were then implanted in rats to repair 10 mm defects of the sciatic nerve. At twelve weeks after implantation, the regenerative outcome of tissue engineered conduits was similar to that of autologous grafts, while both were superior to plain SF/collagen scaffolds, suggesting that the former was able to create a more favorable regenerative microenvironment and could accelerate nerve regeneration. An

alternative fabrication approach was adopted by Zhu et al. [23], who filled a hollow tube made of chitosan with degummed SF fibers. A set of scaffolds was modified with extracellular/acellular matrix and their performance to bridge 10 mm long sciatic nerve gaps in rats was evaluated in comparison with plain chitosan/SF filler scaffolds. It was observed that SF fiber filler promoted deposition of extracellular matrix and that the hybrid scaffold modified with extracellular matrix was more effective in supporting axonal outgrowth from the proximal stump than the unmodified chitosan/SF filler scaffold at both early (2 weeks) and late (12 weeks) regenerative stages.

Besides being biocompatible, biodegradable, and permeable to biological fluids and small molecules, nerve conduits should display an optimum combination of strength and elasticity to withstand clinical operation stresses, such as manipulation and suturing during implantation, to resist deformation and kinking caused by biomechanical *in vivo* stresses, and to avoid channel collapse since compression can result in damage to the growing axon, as well as in pain for the patient. The capability to resist compression is one of the crucial factors for the safe surgical application of nerve conduits. The design of layered architectures for the nerve conduit wall and the combination of biomaterials with different morphologies, chemical, physical, and mechanical properties may help to achieve a balance between the biological and biomechanical performance of a scaffold for nerve regeneration [10,24]. To this aim, we have developed an advanced manufacturing technology able to achieve an effective hybridization between electrospun SF matrices (made of regenerated SF nanofibers) and textile SF matrices (made of native SF microfibers), two materials that share a common chemical composition, but are totally different as regards morphological and physical properties and mechanical performance [25].

This study reports the chemical, morphological, physical, and mechanical characterization of a novel multi-layered SF-based nerve conduit (SFNC), called SilkBridge™. The nerve conduit was produced in different designs: (i) hollow tube ("*SFNC*"), (ii) reinforced hollow tube ("*SFNC+*"), (iii) reinforced tube filled with longitudinally aligned SF microfibers ("*SFNC+/filler*"). The hybrid wall conduit architecture was designed to optimize not only production but also pre-surgery manipulation of the device, suturing at the site of implantation, biological and biomechanical integration with host tissues. *In vitro* cell interaction studies were performed using glial RT4-D6P2T and neuronal NSC-34 cell lines seeded on the conduit. Different parameters were evaluated: proliferation and adhesion for glial cell line and differentiation and neurites elongation for motor neurons cultures. Additionally, *in vivo* preliminary pilot trials in which a 10 mm gap of rat median nerve was repaired with two different SilkBridge™ conduits ("*SFNC+*" and "*SFNC+/filler*" designs) were carried out and the results of histopathological analysis two weeks after implantation are presented and discussed.

2. MATERIALS AND METHODS

2.1 Fabrication of SilkBridge™

The silk fibroin (*Bombyx mori*) nerve conduit (SilkBridge™) is a hybrid three-layered tubular scaffold comprising two electrospun layers (ES, inner and outer), and an intermediate textile layer (TEX). The tubular TEX layer was manufactured using degummed SF yarn (size 40 dtex) by warp needle braiding technology. The ES layers were obtained by electrospinning, using pupae-free silk cocoons as starting material. Cocoons were degummed in autoclave at 120°C for 20 min and extensively washed with warm and cold water. Pure SF fibers were dissolved with an aqueous solution of 9.3 M Lithium Bromide at 60°C for 3 hours. The salt was removed by dialysis and aqueous SF was cast in Petri dishes at 35°C in a ventilated oven until complete evaporation of water. SF films thus obtained were dissolved in Formic Acid (8% w_{SF}/v_{FA}) to prepare the electrospinning dope. Electrospinning was performed as previously reported [26,27], using the following experimental parameters: potential difference = 25 kV, flow rate = 0.8 ml/h, spinneret-collector distance = 14 cm. Coupling of the TEX layer with the two ES layers was made during electrospinning, according to a patented process [25; Supplementary, Scheme S1]. Two different welding media were used: (i) a solution of ionic liquid (1-ethyl-3-methylimidazolium acetate; EMIMAc) in water (EMIMAc/water 80/20% v/v); (ii) a solution of 15% w/w SF in EMIMAc. The tubular scaffolds obtained with EMIMAc/water are identified with the acronym "*SFNC*", while those obtained with EMIMAc/SF with "*SFNC+*". In a design variant the "*SFNC+*" scaffold was filled with 40 degummed SF microfiber yarns with size of 15 dtex each (acronym: "*SFNC+/filler*"). After electrospinning of the two ES layers, as-spun SF nanofibers were consolidated by immersion in aqueous ethanol (80% vol), followed by overnight washing with distilled water and drying. Finished tubular devices were purified by extraction with ethanol to remove processing aids, immersed in distilled water overnight, dried, packaged under laminar flow cabinet and sterilized with ethylene oxide (EtO).

2.2 Morphological, physical, chemical, and mechanical characterization

2.2.1 Scanning Electron Microscopy

Morphological analyses were performed by scanning electron microscopy (SEM) on Au/Pd sputter coated samples (Desk IV, Denton Vacuum, LLC), with a Zeiss EVO MA10 scanning electron microscope at 10 kV acceleration voltage, 100 μA beam current, and 15 mm working distance.

2.2.2 Geometrical properties

Geometrical properties of the tubular scaffolds were determined by measuring the weight per unit length, the wall thickness, the inner diameter, and the porosity of the conduit wall.

Wall thickness was measured according to ISO 7198:2016 standard method. The tubular device was cut longitudinally, flattened and measured with a thickness tester MarCator 1075R (Mahr) equipped with a constant load thickness gauge of 0.3 cm^2 foot area that exerts a pressure of 1 kPa.
Dry state inner diameter was determined from SEM images of tubular cross-sections mounted on stubs, using the SEM software measuring tools.
Porosity was determined according to ISO 7198:2016, using the gravimetric test procedure. A value of 1.35 g/cm^3 was used for the density of the SF material [28].

2.2.3 Attenuated Total Reflectance Fourier Transform Infrared Spectroscopy (ATR-FTIR)

ATR-FTIR was performed with an ALPHA FTIR spectrometer (Bruker) equipped with an ATR Platinum Diamond accessory, at a resolution of 4 cm^{-1}, in the infrared range of 4000-400 cm^{-1}. Spectra were corrected with a linear baseline and normalized to the CH_2 bending peak at about 1445 cm^{-1}. This peak was selected because it is not sensitive to SF molecular conformation.

2.2.4 Differential Scanning Calorimetry (DSC)

Thermal properties were determined by using a calorimeter Netzsch, model DSC 3500 Sirius. Samples (3-5 mg) were closed in Aluminum pans and subjected to a heating cycle from 50°C to 400°C, at a heating rate of 10°C/min, under N_2 atmosphere (flow rate: 20 ml/min).

2.2.5 Compression strength

Compression tests were performed under dry or wet conditions, using an All Electric Dynamic Test Instrument ElectroPuls E3000 (Instron), equipped with a load cell of 250 N, a thermostatic bath (BioPuls), and appropriate grips fabricated *ad hoc* (Supplementary, Scheme S2). Specimens of 10 mm length were mounted on the grips and tested at a crosshead speed of 1.0 mm/min, with a preload of 0.1 N applied before starting the compression cycle. Tests under wet condition were performed with grips fully submersed in water at 37°C. The compression cycle was started after conditioning the specimen for 5 minutes. The force was applied perpendicular to the longitudinal axis of the tubular specimens. Compressive load values were measured at strains of 20%, 40%, and 60%, respectively. Three specimens for each device were analyzed and averaged.

2.3 In vitro cell tests

In vitro cell tests were performed using RT4-D6P2T, a schwannoma cell line (ATCC catalog number CRL-2768) and Mouse Motor Neuron NSC-34 cell Line (Cedarlane catalog number CLU140). SilkBridge™ conduits were cut longitudinally and immersed in phosphate buffer saline (PBS). To allow cell adhesion, the longitudinally open conduits were pressed for a few minutes and then fixed

to the culture plate-well through an insert (Sigma Aldrich, CellCrown™ inserts, catalogue number Z74230). For control conditions, cell lines were plated on not coated glass coverslips.

2.3.1 Proliferation and adhesion assay on RT4-D6P2T cell line

RT4-D6P2T cells were seeded on SilkBridge™ conduits and cultivated in Dulbecco's Modified Eagle Medium (DMEM, Sigma Aldrich) supplemented with 100 U/ml penicillin (Sigma), 0.1 mg/ml streptomycin (Sigma), 1 mM sodium pyruvate (Sigma), 4 mM L-glutamine (Sigma) and 10% heat-inactivated fetal bovine serum (FBS; Invitrogen) at a density of $20x10^3$ cells/cm^2. After 2, 4, and 6 days in vitro (DIV), cells were fixed in 4% paraformaldehyde solution (PFA; Sigma-Aldrich). Fixed cells were permeabilized with 0.1% Triton X-100 for 1 h at room temperature. F-actin was detected using TRITC-conjugated phalloidin diluted 1:1000 in blocking solution (Chemicon-Millipore) by 1 h incubation at room temperature followed by three wash steps of 5 min each and mounted with a Dako fluorescent mounting medium. Images were acquired using a Zeiss LSM800 confocal laser microscopy system (Zeiss, Jena, Germany). For each sample a number of 15 images were taken and the number of cells estimated using Image J software. As regards the cell adhesion, 2 DIV-time point was evaluated, for each image the area of the cell adhesion was evaluated. Experiments were performed as technical and biological triplicates.

2.3.2 Culture of Mouse Motor Neuron NSC-34 cell line

NSC-34 cells were seeded on SilkBridge™ conduits and cultivated in Dulbecco's Modified Eagle Medium (DMEM, Sigma Aldrich) supplemented with 100 U/ml penicillin (Sigma), 0.1 mg/ml streptomycin (Sigma), 4 mM L-glutamine (Sigma) and 10% heat-inactivated fetal bovine serum (FBS; Invitrogen) at a density of $10x10^3$ cells/cm^2. The day after seeding the culture medium was changed in order to promote cell differentiation: DMEM-F12 supplemented with 100 U/ml penicillin, 0.1 mg/ml streptomycin, 4 mM L-glutamine and 1% FBS and Retinoic Acid 1 µM (Sigma).

2.3.3 Immunofluorescence

After 5 days of culture, NSC-34 cells were fixed in 4% PFA for 15 min, washed in 0.1 M phosphate buffer (pH 7.2) and processed for immunofluorescence analysis. Samples were permeabilized, blocked (0.1% Triton X-100, 10% normal goat serum (NGS)/0.1% NaN_3, 1 h) and incubated overnight in anti-βIII-Tubulin (mouse, monoclonal, 1:1000, Sigma-Aldrich) primary antibody; after incubation with secondary antibody goat anti-mouse CY3 (1:200, Molecular Probes, Eugene, Oregon) for 1 h, cells were mounted with a Dako fluorescent mounting medium. Images were acquired using a Zeiss LSM800 confocal laser microscopy system (Zeiss, Jena, Germany). For each

sample 15 images were taken and the number of differentiated and not-differentiated cell and the neurite elongation was estimated using Image J software.

2.4 In vivo pilot study

2.4.1 Animal care

The pilot animal experiment was performed at Neuroscience Institute Cavalieri Ottolenghi (N.I.C.O) stabulary (Ministerial authorization DM 182 2010-A 3-11-2010). The current experimental study has been reviewed and approved by the Ethic Experimental Committee of University of Torino (Ministry of Health project number 864/2016). The study conditions conformed to the guidelines of the European Union's Directive EU/2010/63 for animal experiments. Four adult females Wistar rats, weighing approximately 200 g, were used. Animals were kept under controlled conditions. The animal housing room temperature and relative humidity were recorded daily. The recommended temperature range for the room was between 10°C and 24°C. The light cycle was regulated using an automatic timer (12 h of light, 12 h of dark). The selected animals were healthy and never previously used. They had access to specific food and water ad libitum until 24 h before surgery. Staff involved were properly qualified and trained. Standard veterinary medical care was also provided.

2.4.2 Surgical procedure

In vivo nerve regeneration assays were performed under general anesthesia, Zolazepam (Zoletil, Virban) + Xilazina (Bayer) by intraperitoneal injection (40 mg/kg+5 mg/kg). Median nerves were repaired with SilkBridge™ conduits. The animals received bilateral surgeries and were divided in two experimental groups: (i) nerves were repaired with an empty conduit ("*SFNC+*" design) and withdrawn at 2 weeks (n = 2); (ii) nerves were repaired with a conduit filled with microfibers ("*SFNC+/filler*" design) and withdrawn at 2 weeks (n = 2). Once animals were under anesthesia, the region was shaved and disinfected. Nerve lesion was performed on the median nerves. All surgical procedures were performed under a high magnification surgical microscope, in a clean room.

In both groups, median nerves were transacted, and 12 mm long conduits were used to bridge the nerve defect by inserting 1 mm of the two nerve ends inside the conduit. The nerve conduit was sutured with one 9/0 epineural stitch at each end. The prosthesis was immersed in sterile saline for at least a couple of minutes before implantation.

At day 0, 1, 2, and 3 post-surgery, analgesic therapy with Rymadil (4 mg/Kg, Zoetis Italia) was administered by subcutaneous injection, while at day 2 and 5 post-surgery, the antibiotic treatment (Rubrocillina 0.05 ml/500 g, MSD animal health) was administered by intramuscular injection. After 2 weeks post-operative, rats were sacrificed through anesthetic overdose of Zoletil+Xilazina (> 60 mg/Kg and >10 mg/Kg) by intraperitoneal injection and regenerated nerves analyzed.

2.4.3 Light and confocal microscopy analyses

Regenerated nerve samples, together with the conduit, were fixed by immediate immersion in 4% paraformaldehyde in PBS (Phosphate Buffered Saline) (Sigma) for 2-3 hours at 4°C. For Crio-embedding procedure specimens were rehydrated with PBS (Sigma) and cryo-protected with three passages in increasing solutions of sucrose (Sigma) (7.5% for 1 h, 15% for 1 h, 30% overnight) in 0.1 M PBS. Thereafter, specimens were maintained in a 1:1 solution of sucrose 30% and optimal cutting temperature medium (OCT, electron microscopy sciences) for 30 min and then embedded in 100% OCT. Longitudinal nerve sections were cut at 10 μm and stored at -20°C.

2.4.3.1 Masson's Trichrome Staining

For Masson's trichrome staining a Masson trichrome with aniline blue kit (Bio-Optica) was used: six drops of Weigert's iron hematoxylin (solution A) and six drops of Weigert's iron hematoxylin (solution B) were combined together and used to stain slides for 10 min. Without washing, the slides were then drained and incubated with ten drops of alcoholic picric acid solution for 4 min. After washing in distilled water, sections were stained with ten drops of Ponceau acid fuchsin for 4 min and washed again in distilled water. Further on, ten drops of phosphomolybdic acid solution were added to the section for 10 min. Without washing, the slides were drained, and 10 drops of aniline blue were added to the section for 5 min. Finally, after washing in distilled water, dehydrating rapidly in ethanol and clearing in xylol/Bioclear (Bio-Optica), the slides were mounted in DPX (Fluka).

2.4.3.2 Immunohistochemistry

The sections were rinsed in PBS, blocked with normal serum (1% in PBS-Triton 0,1%) for 1 h and then incubated overnight with the primary antibody. After primary antibody(ies) incubation, sections were washed three times in PBS and incubated for 1 h in a solution containing the secondary antibody(ies): Alexa 488 anti-Mouse, Cy3 anti-Rabbit (Life Technologies) conjugated with a fluorophore and selected in order to recognize the species of primary antibodies. After three washes in PBS, sections were finally mounted with a Dako fluorescent mounting medium and stored at 4°C before being analyzed.

Both axon and glia can be detected by immunohistochemistry using specific antibodies. Sections were incubated in a solution containing the following primary antibodies, used alone or in pairs: (*i*) anti-NF 200 kDa (monoclonal, mouse, Sigma Aldrich); (*ii*) S-100 (polyclonal, rabbit, Sigma Aldrich).

2.4.4 High resolution light microscopy and electron microscopy analyses

Regenerated nerve samples, together with the conduit, were fixed by immediate immersion in 2.5% glutaraldehyde (SIC, Società Italiana Chimici) in 0.1 M phosphate buffer (pH 7.4) for 5-6 h, at 4°C. Samples were then post-fixed in 2% osmium tetroxide (SIC, Società Italiana Chimici) for 2 h and

dehydrated in passages in ethanol (Sigma Aldrich) from 30% to 100% (5 minutes each passage). After two passages of 7 min in propylene oxide and overnight in a 1:1 mixture of propylene oxide (Sigma Aldrich) and Glauerts' mixture of resins, samples were embedded in Glauerts' mixture of resins (made of equal parts of Araldite M and the Araldite Harter, HY 964, Sigma Aldrich). In the resin mixture, 0.5% of the plasticizer dibutyl phthalate (Sigma Aldrich) was added. For the final step, 2% of accelerator 964 was added to the resin in order to promote the polymerization of the embedding mixture, at 60°C.

Semi-thin sections (2.5 μm thick) were cut using an Ultracut UCT ultramicrotome (Leica Microsystems, Wetzlar, Germany) and stained with 1% toluidine blue for high resolution light microscopy examination and design-based stereology. A DM4000B microscope equipped with a DFC320 digital camera and an IM50 image manager system (Leica Microsystems, Wetzlar, Germany) was used for section analysis. With the same ultramicrotome, ultra-thin sections (70 nm thick) were cut. Sections were analyzed using a JEM-1010 transmission electron microscope (JEOL, Tokyo, Japan) equipped with a Mega-View-III digital camera and a Soft-Imaging-System (SIS, Münster, Germany) for the computerized acquisition of the images.

2.4.5 Statistical analysis

For the *in vitro* experiments statistical analysis was performed using Two-Sample t-Test. Statistical analysis were performed using SPSS Software. The level of significance was set at $p \leq 0.05$ (*), $p \leq 0.01$ (**), and $p \leq 0.001$ (***). Values were expressed as mean ± SEM.

3. RESULTS

3.1 Morphological characterization

The SilkBridge™ conduit is made of two electrospun layers (ES, inner and outer) coupled with an intermediate textile (TEX) layer (Figure 1, A-E). Both ES and TEX layers are made of pure SF, from which sericin was completely eliminated. Two different approaches were used to weld the ES and TEX layers during electrospinning. In one case ("*SFNC*" design), EMIMAc/water solution was used as welding medium. After consolidation and washing, the surface of SF microfibers remained as clean and smooth as native ones (Figure 1, F - left panel). In the other case ("*SFNC+*" design), coupling was performed with EMIMAc containing SF dissolved in it. After consolidation/washing, this welding medium left a thin SF film onto the surface of microfibers, which stuck them together and made the yarn texture more rigid and compact (Figure 1, F - right panel).

The geometrical properties of SilkBridge™ conduits are listed in Table 1. A nerve conduit with an inner diameter of 1.65 mm and a wall thickness of 0.52 mm has a weight per unit length of only ~8

mg/cm. The light weight is favored by the open structure of the braided mesh forming the TEX layer (Figure 1, D). The value of wall porosity of about 80% is the combination of macro- and micro-porosity of the TEX and ES layers, respectively, and falls in the optimal range reported for peripheral nerve repair [10].

3.2 Physical-chemical characterization

Spectroscopic properties of SilkBridge™ conduits were characterized by ATR-FTIR. Figure 1, G shows typical spectra of ES and TEX layers. Position, shape, and intensity of the conformationally sensitive Amide bands (Amide I at 1625 cm^{-1}, with shoulder at 1695 cm^{-1}; Amide II at 1517 cm^{-1}; Amide III at 1231 cm^{-1} and 1264 cm^{-1}) show that both native (TEX layer) and regenerated (ES layer) components display a β-sheet crystalline structure [26,29]. The crystallinity of SF nanofibers was calculated from the intensity ratio between the two Amide III components at 1231 cm^{-1} and 1264 cm^{-1} ($CI = I_{1264}/I_{1231}$). An average CI value of 0.57 was obtained, similar to that of native microfibers ($CI \cong 0{,}60$) [29].

Thermal properties of SilkBridge™ conduits were investigated by DSC analysis. Figure 1, H shows typical thermograms of the TEX layer, ES layer, and of the hybrid three-layered tubular device. The TEX layer displays a high thermal stability, with a main endothermic transition peaking at about 320°C, attributed to melting/degradation of highly crystalline and oriented native SF microfibers [29]. The ES layer, likewise many other regenerated SF materials, shows a marked low-temperature shift of the same transition, with a main peak at about 289°C [26]. The DSC profile of the finished device is the sum of the individual components, with two peaks corresponding to the characteristic thermal transitions of ES and TEX layers.

The ES:TEX weight ratio was calculated from the relative intensity of the respective DSC endotherms. Using the enthalpy (ΔH) values of -402 ± 41 J/g and -307 ± 32 J/g for TEX and ES layers, respectively, the weight contribution of each component in the three-layered scaffold was calculated and reported in Table 1. The results show that the inner and outer ES layers account for about 59% by weight, while the remaining 41% is due to the weight contribution TEX layer.

3.3 Mechanical characterization

The impact of the different manufacturing designs ("*SFNC*", "*SFNC+*", "*SFNC+/filler*") on the mechanical properties of the tubular scaffold was studied by measuring the compression strength under dry and wet conditions. Values of compressive load were recorded at three levels of strain (20%, 40%, and 60%) and listed in Table 2. As expected, the overall values recorded under dry conditions were significantly larger than those obtained with the scaffold submersed in water at 37°C.

The "*SFNC+*" design achieved higher compression resistance owing to the presence of the reinforcing SF film left by the welding medium on the surface of TEX microfibers.

Under wet conditions, both the "*SFNC+*" and "*SFNC+/filler*" designs performed constantly better than the SFNC at all strain values, thus confirming that the presence of the SF film enhanced the mechanical performance of the tubular scaffold. The high compression strength of the "*SFNC+/filler*" design at 60% strain was due to the presence of the filler which reduced the lumen empty space. Based on these results, the "*SFNC*" design was discarded while "*SFNC+*" and "*SFNC+/filler*" designs were selected to carry out *in vivo* testing on animal model.

3.4 *In vitro* biomimetic properties evaluation

Direct contact assays of glial RT4-D6P2T and neuronal NSC-34 cell lines cultured on the luminal surface of SilkBridge™ conduits cut lengthwise ("*SFNC+*" design) were conducted to evaluate the biocompatibility and the biomimeticity of the biomaterial. The glial cells model was used to evaluate the proliferation profile after 2, 4, and 6 days of culture and adhesion at 2 days-time point. The results of direct contact assays (Figure 2) showed that SilkBridge™ is capable to sustain cell proliferation. Although cells grown on the control substrate showed a more marked replicative capacity, cells grown on the luminal surface of the conduit were able to increase their density by at least 6 times at each time point. Moreover, RT4-D6P2T cells grown on SilkBridge™ showed a very well-organized morphology with a typical F-actin organization characterized by stress-fibers, indicating an excellent cell adhesion (Figure 2, B-D-F) and a statistically greater dimension than cells grown on control substrates (Figure 2, H).

The biomimetic attitude of SilkBridge™ in sustaining phenomena such as differentiation and nervous sprouting was assessed with NSC-34 cell line (Figure 3, B-D-F) and compared with the same cells grown and differentiated on a control substrate (Figure 3, A-C-E). One day after plating, cells were subjected to the protocol of differentiation. The ratio between the differentiated and non-differentiated neurons reflects the one observed in the controls, in fact no statistical significance was observed between the two experimental groups (Figure 3, G). However, the analysis of the length of the neurites developed both on control substrate and on SilkBridge™ showed a more pronounced tendency to elongation in samples of NSC-34 cultivated on SilkBridge™ with respect to controls (Figure 3, H).

3.5 *In vivo* pilot experiments on nerve regeneration

3.5.1 Surgical procedures, macroscopic evaluations and animal welfare

During surgeries, the behavior of the nerve conduits was evaluated. The conduit has proven to be easily to handle, adequately flexible and easily suturable. No signs of collapse were observed. The implantation area was evaluated during the period following the surgery and the aspect of the surgical wound appeared normal and without signs of inflammation. All animals survived the experimental period and were in good health condition throughout the experiment. No signs of pain, discomfort or auto-mutilation were reported in any of them. At the time of explantation (two weeks) all conduits were still clearly distinguishable and were found on site. They were covered with a thin layer of connective tissue. No signs of inflammation or scar tissue formation around the conduit was detected, demonstrating its biocompatibility (Figure 4).

3.5.2 Histopathological and immunological approach

To observe the qualitative morphology of the nerve in the early stages of regeneration, both longitudinal and transversal sections were analyzed. In particular, longitudinal sections underwent Masson's trichrome staining and immunofluorescence staining in order to have a macroscopical overview of the early stage of regeneration; semithin toluidine-blue stained cross sections and thin cross sections were analyzed by high resolution light microscopy and electron microscopy, respectively, in order to study the microscopical behavior of regenerated nerves. All analyses were carried out at short-term time point post-surgery (2 weeks). Cross-section images were gathered inside the graft, both proximally and distally, to follow nerve regeneration alongside the conduits.

3.5.2.1 Median nerve repaired with SilkBridge™: "SFNC+/filler" design

Trichrome staining of longitudinal sections showed the presence of a thin layer of connective tissue surrounding the outer side of the conduit (Figure 5, A). At two weeks from surgery, several cell types colonized the lumen of the conduit (Schwann cells, fibroblasts, cells of the immune system) (Figure 5, B). The middle portion of the conduit was not yet colonized by cells or extracellular matrix, meaning that cells have still to migrate in the central part of the conduit. At higher magnification it was possible to appreciate the interaction between cells and fibroin fibers (Figure 5, C). Interestingly, regenerated nerve fibers are already detectable in the proximal portion of the tube by immunofluorescence analysis: double immunostaining with neuronal marker (neurofilament) and glial marker (S-100) showed the presence of regenerated nerve fibers associated with Schwann cells (Figure 5, D-E).

With high resolution light microscopy on transversal nerve section it was possible to observe the behavior of the SF microfibers inserted as filler inside the conduit: cross-section images showed that

they are packed to one side of the conduit, leaving the other side without fibers (Figure 6, A-B-C). Cells and blood vessels were also visible between the different layers of the conduit wall (Figure 6, D-E). Electron microscopy analysis showed the presence of few regenerated myelinated fibers with a thin myelin sheath at proximal level (Figure 6, F-G), whereas at distal level no myelinated fibers were detected yet.

3.5.2.2 Median nerve repaired with SilkBridge™: "SFNC+" design

The morphological analysis of median nerve repaired with the empty conduit showed similar results compared to those observed with the conduit filled with microfibers, i.e.: (*i*) a thin layer of connective tissue surrounding the outer side of the conduit (Figure 7, A); (*ii*) a rich cellular colonization proximally and distally (Figure 7, B-C); (*iii*) a still empty middle portion of the conduit; (*iv*) nerve fibers already detectable in the proximal portion of the tube; (*v*) the presence of regenerated nerve fibers associated with Schwann cells (Figure 7, D-E).

High resolution images of transversal cross-sections displayed extensive cellular colonization at proximal and distal levels, as well as between the layers of the conduit wall, with several cell types and many blood vessels (Figure 8, A-E). Neurofilament positive regenerated myelinated fibers with a thin myelin sheath were detectable only in the distal portion of the tube (Figure 8, F-G).

4. DISCUSSION

A wide range of materials have been studied and tested for the repair of peripheral nerve injuries with substance loss, including synthetic non-resorbable polymers (silicone, polyethylene glycol), synthetic resorbable polymers (polyglycolic acid - PGA; polycaprolactone - PCL), and biopolymers (chitosan, silk fibroin, collagen). The resulting picture often presents lights and shadows, as there are many advantages and adverse effects of their use in the repair of nerve gaps. Silicone tubes are not permeable to large molecules resulting in a possible fibrotic capsule formation around the guide. Resorbable PGA conduits in some cases displayed too short degradation time, not enough for complete nerve regeneration. Moreover, their degradation into lactic acid may be harmful for the biological microenvironment of the site of implantation. Interestingly, the use of copolymers with PCL decreased the impact of this problem and led to long-term *in vivo* histological outcomes comparable to autograft but entailed a greater rigidity and a more difficult handling of the device [30]. Actually, an optimum balance between morphological, mechanical, biological, and functional properties of a scaffold for nerve repair and regeneration may be difficult to achieve because some excellent properties are often accompanied by structural and/or functional gaps that may compromise all or part of the performance of the device itself. In this context, our ambition is to overcome the current limitations by taking full advantage of the excellent characteristics of silk fibroin [12-14,31].

This biomaterial offers high versatility in matrix scaffold design for a number of biomedical needs in which mechanical performance and biological interactions are major factors for success. The mechanical properties, as well as the rate of degradation of an SF scaffold can be finely tuned by selecting and combining appropriate manufacturing methods. SF materials usually display appropriate interactions with cells and living tissues. A mild inflammatory response that decreases within a few weeks of implantation is often observed, allowing for vascularization, tissue remodeling, tissue ingrowth with eventual complete replacement by native tissue. The strengths of using silk for the production of nerve conduits will be detailed in the following discussion.

The novel SilkBridge™ conduit is a hybrid tubular structure consisting of two electrospun layers (ES) coupled with an intermediate textile layer (TEX). Its fabrication is based on a patented technology that allows the production of hybrid tubular structures which combine the outstanding mechanical properties of native SF microfibers and the enhanced biomimicking attitude of regenerated SF nanofibers [25]. The fabrication technology was progressively refined through recursive testing and optimization procedures which led to a standardized production protocol. Great attention was devoted to the careful selection of starting materials and processing aids, as well as to the fine-tuning of key processing parameters. In particular, the optimized coupling strategy leads to a hybrid structure where the ES and TEX layers are perfectly integrated at the structural and functional level, and respond as a single body to mechanical stresses, without showing slipping or separation between adjacent layers, thus making easier manipulation and suturing during surgery, and avoiding the emergence of biomechanical mismatch at the implantation site.

The SilkBridge™ nerve conduit can be produced in a wide range of inner diameter and length, to cover all needs for clinical application. The combined use of different SF-based materials, i.e. the thin and microporous ES layers encasing the strong SF braided mesh with an open texture characterized by the presence of macroscopic voids, results in a light weight, porous, mechanically resistant, biodegradable, and biocompatible scaffold able to meet key requirements for *in vivo* nerve regeneration [8,10]. The light weight of the device, about three times lower than that of a similar commercial nerve conduit made of chitosan (Reaxon® Nerve Guide), does not seem to negatively impact on its mechanical properties, as discussed below, but it is likely to bring biological advantages because the load of foreign material at the site of implantation is significantly reduced, thus avoiding excessive physiological stresses to surrounding tissues during remodeling.

An important function of nerve conduits is to provide support to the regenerating axon by hosting nerve cell populations, maintaining cell proliferation and differentiation, permitting nutrients, oxygen, and metabolites transport and exchange with the surrounding environment, while preventing infiltration of inflammatory cells inside the conduit as well as outflow of the growth factors secreted

by the distal nerve stump. All these features are under the control of geometric parameters of the nerve conduit wall such as thickness, porosity, and pore size. Kokai et al. [32] reported that wall thickness and porosity values of about 0.6 mm and 80%, respectively, allow permeation of small nutrient molecules and prevent larger molecules (e.g. lysozyme) and cells from diffusing inside the conduit, thus optimizing the conditions for nerve regeneration. Both wall thickness and porosity values of SilkBridge™ fall in the desired range of well performing nerve conduits. The optimum range of pore size has been less defined in previous studies, spanning from few micrometers up to 30 μm [8]. Sarazin et al. [33] reported that 20 μm may be a critical limit for cell infiltration. Actually, the double electrospun layers comprising the wall of the SilkBridge™ conduit ensure a high porosity level in the low pore size range [34], which can be considered safe for the permeability of small molecules, while hinders large molecules and cells from invading the lumen of the conduit.

A crucial role in the axonal regeneration process is played by the biomechanical response of the tubular conduit, in particular by the capability to resist to compression stresses to which it might be exposed at the site of implantation. Therefore, the relation between compressive resistance and morphological and geometrical features of the scaffold must be investigated and compressive resistance must be carefully measured. Despite the extensive scientific literature on SF-based nerve conduits, to our best knowledge very few papers reported data on compressive performance. Yang et al. [35] manufactured a SF-based nerve conduit by using the injection molding technique; geometrical parameters were similar to the scaffold of the present study, i.e.: inner diameter = 1.6 mm; wall thickness = 0.75 mm. To overcome the weakness and fragility of SF spongy materials obtained by lyophilization, a reinforcement made of SF microfibers was wrapped around the central cylinder of the mold before injecting the SF solution. The mechanical strength of the composite scaffold was then evaluated in the compression mode. Authors reported a maximum compression strength in the wet state of about 0.025 N, a value lower than that obtained for the different SilkBridge™ designs here reported.

Higher compression values in the wet state were reported by Wu et al. [36], who prepared a nerve conduit made of a polymer blend of SF and chitosan–poly(p-dioxanone) copolymer cross-linked with genipin, by using the injection molding technique. Maximum compression values in the range 120-140 N/m at 60% strain were reported and were considered satisfactory for the performance requirements of a nerve conduit scaffold, which must be able to withstand tissue compression arisen from muscle contraction, joint movement, and body weight for the time needed to regenerate a new axon. Despite the differences in manufacturing technology, geometrical parameters, and 3D architecture, the values of compression strength at 60% strain of the best performing SilkBridge™

designs ("*SFNC+*" and "*SFNC+/filler*") are higher (see: Table 2). The compression modulus was estimated from the initial slope of the load/strain curves and a value of 0.51 MPa was obtained. Noteworthy, this value is higher than those reported by Madduri et al. [37] for a couple of commercial nerve conduits, i.e. the collagen-based Neuragen® (0.08 MPa) and the poly(DL-lactide-co-caprolactone)-based Neurolac® (0.14 MPa). These results allow concluding that the best performing SilkBridge™ design meets the mechanical performance requirements for clinical application, being able to withstand reported physiological and pathological compressive stresses, e.g. 0.004 MPa for nerves in common functional position and 0.015 MPa for the carpal tunnel syndrome with the nerve in full extension [38].

Biodegradable nerve conduits are generally more promising in bridging nerve gaps as they can degrade after accomplishing their task [39]. However, there is unanimous consensus that the degradation profile of a nerve conduit should be complementary to the growth rate of the regenerating nerve [10]. Mismatch between scaffold degradation and axonal re-growth might have serious consequences on the course of the healing process. SilkBridge™ is made of both native and regenerated SF components. The medium-to-long term degradation profile (1-2 years) of native SF fibers is well known [13]. On the other hand, regenerated SF materials such as electrospun nanofibers are characterized by short-to-medium term degradation profiles (from weeks to months) depending on the manufacturing protocol used and processing conditions [12]. As-spun regenerated SF nanofibers of SilkBridge™ underwent various consolidation steps with hydro-alcoholic solutions aimed at inducing β-sheet crystallization. The determination of the spectroscopic crystallinity index confirmed the completion of the conformational transition from random coil to highly crystalline SF nanofibers, with a high crystal content, similar to that reported for native microfibers [29]. This parameter is very important for the functionality of the device, because the degree of crystallinity of regenerated SF materials has a strong influence on the rate of *in vivo* biodegradation [14]. In fact, highly crystalline regenerated SF materials proved to be more favorable to ensure low degradation rate in the biological environment [40]. In our case, the ES nanofiber layers forming the wall of SilkBridge™ are expected to undergo remodeling in the medium term, while long-term biomechanical support will be ensured by the native silk fibers comprising the TEX layer, thus allowing enough time for achieving full axonal regeneration.

The study of the biological properties of the SilkBridge™ nerve conduit comprised both *in vitro* and *in vivo* tests, with the aim to evaluate the biocompatibility of the device and to assess the ability to sustain the repair of peripheral nerve injury in a standardized murine pre-clinical model. *In vitro* biocompatibility was evaluated by seeding glial RT4-D6P2T and neuronal NSC-34 cell lines on the

luminal surface of the longitudinally open hollow tube ("*SFNC+*" design), while the pilot *in vivo* trial was conducted using both "*SFNC+*" and "*SFNC+/filler*" designs.

The results of *in vitro* tests demonstrated that both cell lines adhered and proliferated efficiently on the SF nanofibrous substrate of the SilkBridge™ wall. In particular, RT4-D6P2T cells showed a very well organized glial-like cell morphology, while neuronal NSC-34 cells differentiated and achieved an enhanced neurites length compared to the same cells grown on control substrate. These data are in good agreement with previous studies, where the *in vitro* biocompatibility of either native [41,42] or regenerated [34,43-47] SF substrates, including electrospun mats, was tested with different cells of the nervous system. Dorsal root ganglia cells closely adhered to SF fibers at short culture times and showed neurite outgrowth and axon bundles running parallel to them at longer times [41]. Tang et al. [42] demonstrated that native SF fibers supported survival and growth of hippocampal neurons, which showed viability levels and morphological features closely similar to neurons cultivated in plain neuronal medium. Electrospun SF scaffolds fabricated with formic acid were beneficial to adhesion and proliferation of Schwann cells without exerting any significant cytotoxic effects on their phenotype [34,43]. A lyophilized SF multichannel scaffold produced by molding sustained adhesion, proliferation and directional extension of hippocampal neurons, which also expressed marker proteins and formed 3D neuronal networks *in vitro* [44]. Sagnella et al. [45] highlighted the influence of processing parameters on the physical and chemical properties of regenerated SF substrates (films) and on their interaction with neural cells. In particular, more hydrophobic surfaces enhanced proliferation of astrocytes and adhesion of neuron, while more hydrophilic surfaces remarkably promoted neurite outgrowth. All these experimental data, including those reported in the present study, confirm that various formats of SF-based substrates, from native fibers to regenerated nanofibers, are highly biocompatible towards neural cells and provide a permissive environment for cells to grow on, differentiate and start the fundamental cellular regenerative activities.

The aim of the *in vivo* pilot study of SilkBridge™ nerve conduit was twofold, on the one hand to select the optimal design to be used for the future medium-to-long term trials (empty conduit or conduit with fibers filler), on the other hand to verify the *in vivo* behavior of the conduit in terms of biocompatibility, biomimeticity and non-toxicity. A pilot study at short time point is necessary and essential when moving from *in vitro* to long-term *in vivo* experiments. Indeed, the nerve tissue is a very complex tissue and *in vitro* experiments are useful but not totally predictive in assessing the characteristics of a newly-designed nerve prosthesis in terms of the behavior with the different cells types that eventually colonize it and of the response of surrounding tissues. The study was performed on rats, a standardized animal model widely employed in nerve regeneration studies for various reasons: the anatomy of rat nerves is well established and, in general, very similar to human anatomy;

the size of rat nerves reduces the complexity of the microsurgical procedures; standardized and reliable functional tests are available. The sciatic nerve is the most widely used nerve reconstruction model; many plain SF scaffolds for nerve repair have been tested using a 10 mm sciatic nerve gap as surgical procedure [19,20,34,35,46,47]. However, we preferred to perform the surgical operation on the median nerve, more complex to operate but more favorable in terms of effective functional evaluation (the simple and reliable behavioral grasping test can be executed) and because autotomy has never been reported as side-effect [48]. The two SilkBridge™ designs implanted in rats ("*SFNC+*": hollows tube; "*SFNC+/filler*": same tube filled with SF fibers) demonstrated, at 2 weeks' time point, similar effects on the early stages nerve regeneration processes: (*i*) good integration with the surrounding tissues; (*ii*) formation of a thin layer of connective tissue surrounding the outer side of the conduit; (*iii*) absence of scar formation; (*iv*) colonization of the wall layers and of the lumen with several cell types; (*v*) formation of many blood vessels; (*vi*) presence of few regenerated myelinated fibers with a thin myelin sheath at the proximal nerve stump. All these features highlight the starting of regenerative processes mediated by the SilkBridge™ conduit. This biological behavior, which is under verification with medium-to-long term *in vivo* studies on the same animal model, is an important achievement for the further development of this newly designed SF-based nerve conduit, which is intended as an "off-the-shelf" device to be used as it is, without the need of adding neurotrophic and/or angiogenic factors or cells.

5. CONCLUSIONS

The hybrid multilayered SilkBridge™ nerve conduit showed an optimized balance between biomechanical and biological properties, complementing the high resistance to mechanical stresses of native SF microfibers and the enhanced biomimicking attitude of SF nanofibers. The manufacturing technology resulted in a novel 3D architecture, which allowed achieving an effective hybridization between electrospun and textile SF matrices. Both electrospun and textile layers comprising the conduit wall were perfectly integrated at the structural and functional level, thus avoiding the emergence of biomechanical mismatch during the surgical procedure and at the implantation site. The combined use of native and regenerated SF materials not only conferred high porosity and high compression strength on the SilkBridge™ conduit, but also allowed designing a device with a biodegradation profile covering the clinical time scale for safe and complete axonal regeneration and functional recovery. Both *in vitro* and *in vivo* results demonstrated that SilkBridge™ nerve conduit is a biocompatible and biomimetic substrate for cells to grow on. *In vitro* analysis revealed that nervous cells are able to differentiate and start the fundamental cellular regenerative

activities, while *in vivo* studies showed, at short time-point, a perfect cellular colonization of the conduit and the progressive growth of the regenerating nerve fibers. The promising results of the *in vivo* pilot tests here reported are under verification with on-going preclinical trials, using the autologous nerve repair approach as control. The preliminary feedbacks on functional recovery are very encouraging and the complete set of histopathological and functional results will be reported soon.

Acknowledgements

This research did not receive any specific grant from funding agencies in the public, commercial, or not-for-profit sectors.

Disclosures

Conflict of interest statement: the study is sponsored by Silk Biomaterials srl; G. Freddi and A. Alessandrino are stock owners and employees of the sponsoring organization; G. Bassani, M. Biagiotti, and V. Vincoli are employees of the sponsoring organization; F. Fregnan, L. Muratori, G. Ronchi, and S. Geuna are consultants of the sponsoring organization; P. Pierimarchi is a former member of the Board of Directors of the sponsoring organization.

Data Availability

The raw/processed data required to reproduce these findings cannot be shared at this time as the data also forms part of an ongoing study.

REFERENCES

[1] M.A. Ferrante. The Assessment and Management of Peripheral Nerve Trauma. Curr Treat Options Neurol 20 (2018) 25. DOI: 10.1007/s11940-018-0507-4

[2] S.B. Habre, G. Bond, X.L. Jing, E. Kostopoulos, R.D. Wallace, P. Konofaos. The Surgical Management of Nerve Gaps. Present and Future. Ann Plast Surg 80 (2018) 252-261. DOI: 10.1097/SAP.0000000000001252

[3] J.R. Fowler, M. Lavasani, J. Huard, R.J. Goitz. Biologic Strategies to Improve Nerve Regeneration after Peripheral Nerve Repair. J Reconstr Microsurg. 31 (2015) 243-248. DOI: 10.1055/s-0034-1394091

[4] E.N. Bontioti, M. Kanje, and L.B. Dahlin. Regeneration and functional recovery in the upper extremity of rats after various types of nerve injuries. Journal of the Peripheral Nervous System. 8 (2003) 159-168. DOI: 10.1046/j.1529-8027.2003.03023.x

[5] J.-L. Shen, Y.-S. Chen, J.-Y. Lin et al. Neuron regeneration and proliferation effects of danshen and tanshinone IIA. Evidence-Based Complementary and Alternative Medicine. 211 (2011). DOI: 10.1155/2011/378907

[6] R. Donzelli, C. Capone, F.G. Sgulò, G. Mariniello, F. Maiuri. Vascularized nerve grafts: an experimental study. Neurological Research 38 (2016) 669-677. DOI: 10.1080/01616412.2016.1198527

[7] S. Yi, L. Xu, X. Gu. Scaffolds for peripheral nerve repair and reconstruction. Experimental Neurology (2018). DOI: 10.1016/j.expneurol.2018.05.016

[8] V. Chiono, C. Tonda-Turo. Trends in the design of nerve guidance channels in peripheral nerve tissue engineering. Progress in Neurobiology 131 (2015) 87-104. DOI: 10.1016/j.pneurobio.2015.06.001

[9] S. Madduri, B. Gander. Growth factor delivery systems and repair strategies for damaged peripheral nerves. Journal of Controlled Release 161 (2012) 274-282. DOI: 10.1016/j.jconrel.2011.11.036

[10] A.R. Nectow, K.G. Marra, D.L. Kaplan. Biomaterials for the Development of Peripheral Nerve Guidance Conduits. Tissue Engineering: Part B 18 (2012) 40-50. DOI: 10.1089/ten.teb.2011.0240

[11] X. Gu, F. Ding, Y. Yang, J. Liu. Construction of tissue engineered nerve grafts and their application in peripheral nerve regeneration. Progress in Neurobiology 93 (2011) 204–230. DOI: 10.1016/j.pneurobio.2010.11.002

[12] D.N. Rockwood, R.C. Preda, T. Yücel, X. Wang, M.L. Lovett, D.L. Kaplan. Materials fabrication from Bombyx mori silk fibroin. Nature Protocols 6 (2011) 1612-1631. DOI:10.1038/nprot.2011.379

[13] G.H. Altman, F. Diaz, C. Jakuba, T. Calabro, R.L. Horan, J. Chen, H. Lu, J. Richmond, D.L. Kaplan. Silk-based biomaterials. Biomaterials 24 (2003) 401-416. DOI: 10.1016/S0142-9612(02)00353-8

[14] A.E. Thurber, F.G. Omenetto, D.L. Kaplan. In vivo bioresponses to silk proteins. Biomaterials 71 (2015) 145-157. DOI: 10.1016/j.biomaterials.2015.08.039

[15] M. Farokhi, F. Mottaghitalab, M.A. Shokrgozar, D.L. Kaplan, H.-W. Kim, S.C. Kundu. Prospects of peripheral nerve tissue engineering using nerve conduit conduits based on silk fibroin protein and other biopolymers. International Materials Reviews 62 (2017) 367-391. DOI: 10.1080/09506608.2016.1252551

[16] C. Xue, H. Zhu, D. Tan, H. Ren, X. Gu, Y. Zhao, P. Zhang, Z. Sun, Y. Yang, J. Gu, Y. Gu, X. Gu. Electrospun silk fibroin-based neural scaffold for bridging a long sciatic nerve gap in dogs J Tissue Eng Regen Med (2017). DOI: 10.1002/term.2449

[17] X. Tang, C. Xue, Y. Wang, F. Ding, Y. Yang, X. Gu. Bridging peripheral nerve defects with a tissue engineered nerve graft composed of an in vitro cultured nerve equivalent and a silk fibroin-based scaffold. Biomaterials 33 (2012) 3860-3867. DOI: 10.1016/j.biomaterials.2012.02.008

[18] Y. Zhang, J. Huang, L. Huang, Q. Liu, H. Shao, X. Hu, L. Song. Silk Fibroin-Based Scaffolds with Controlled Delivery Order of VEGF and BDNF for Cavernous Nerve Regeneration. ACS Biomater. Sci. Eng. 2 (2016) 2018-2025. DOI: 10.1021/acsbiomaterials.6b00436

[19] M. Ebrahimi, J. Ai, E. Biazar, S. Ebrahimi-Barough, A. Khojasteh, M. Yazdankhah, S. Sharifi, A. Ai, S. Heidari-Keshel. In vivo assessment of a nanofibrous silk tube as nerve conduit for sciatic nerve regeneration, Artificial Cells, Nanomedicine, and Biotechnology (2018) DOI: 10.1080/21691401.2018.1426593

[20] Y. Yang, X. Yuan, F. Ding, D. Yao, Y. Gu, J. Liu, X. Gu. Repair of Rat Sciatic Nerve Gap by a Silk Fibroin-Based Scaffold Added with Bone Marrow Mesenchymal Stem Cells. Tissue Engineering: Part A 17 (2011) 2231-2244. DOI: 10.1089/ten.tea.2010.0633

[21] C. Wang, Y. Jia, W. Yang, C. Zhang, K. Zhang, Y. Chai. Silk fibroin enhances peripheral nerve regeneration by improving vascularization within nerve conduits. J Biomed Mater Res Part A 106A (2018) 2070-2077. DOI: 10.1002/jbm.a.36390

[22] Y. Xu, Z. Zhang, X. Chen, R. Li, D. Li, S. Feng. A Silk Fibroin/Collagen Nerve Scaffold Seeded with a Co-Culture of Schwann Cells and Adipose-Derived Stem Cells for Sciatic Nerve Regeneration. PLoS ONE 11 (2016) e0147184. DOI: 10.1371/journal.pone.0147184

[23] C. Zhu, J. Huang, C. Xue, Y. Wang, S. Wang, S. Bao, R. Chen, Y. Li, Y. Gu. Skin derived precursor Schwann cell-generated acellular matrix modified chitosan/silk scaffolds for bridging rat sciatic nerve gap. Neuroscience Research 135 (2018) 21-31. DOI: 10.1016/j.neures.2017.12.007

[24] Y. Wang, X. Gu, Y. Kong, Q. Feng, Y. Yang. Electrospun and woven silk fibroin/poly(lactic-co-glycolic acid) nerve guidance conduits for repairing peripheral nerve injury. Neural Regeneration Research 10 (2015) 1635-1642. DOI: 10.4103/1673-5374.167763

[25] A. Alessandrino. Process for the production of a hybrid structure consisting of coupled silk fibroin microfibers and nanofibers, hybrid structure thus obtained and its use as implantable medical device. WO 2016/067189 A1

[26] B. Marelli, A. Alessandrino, S. Farè, M.C. Tanzi, G. Freddi. Electrospun silk fibroin tubular matrixes for small vessel bypass grafting. Materials Technology 24 (2009) 52-57. DOI: 10.1179/175355509X417945

[27] B. Marelli, A. Alessandrino, S. Farè, G. Freddi, D. Mantovani, M.C. Tanzi. Compliant electrospun silk fibroin tubes for small vessel bypass grafting. Acta Biomaterialia 6 (2010) 4019–4026. DOI: 10.1016/j.actbio.2010.05.008

[28] S.A. Fossey, D.L. Kaplan. Silk protein. In: Polymer Data Handbook, by J.E. Mark, 1999, Oxford University Press, Inc.

[29] A. Chiarini, G. Freddi, D. Liu, U. Armato, I. Dal Prà. Biocompatible silk noil-based three-dimensional carded-needled nonwoven scaffolds conduit the engineering o novel skin connective tissue. Tissue Engineering: Part A 22 (2016). DOI: 10.1089/ten.tea.2016.0124

[30] A.J. Reid, A.C. de Luca, A. Faroni, S. Downes, M. Sun, G. Terenghi, P.J. Kingham. Long term peripheral nerve regeneration using a novel PCL nerve conduit. Neurosci Lett 544 (2013) 125-130. DOI: 10.1016/j.neulet.2013.04.001

[31] I. Dal Prà, G. Freddi, J. Minic, A. Chiarini, U. Armato. De novo engineering of reticular connective tissue in vivo by silk fibroin nonwoven materials. Biomaterials 26 (2005) 1987-1999. DOI: 10.1016/j.biomaterials.2004.06.036

[32] L.E. Kokai, Y.-C. Lin, N.M. Oyster, K.G. Marra. Diffusion of soluble factors through degradable polymer nerve guides: Controlling manufacturing parameters. Acta Biomaterialia 5 (2009) 2540-2550. DOI: 10.1016/j.actbio.2009.03.009

[33] P. Sarazin, X. Roy, B.D. Favis. Controlled preparation and properties of porous poly(l-lactide) obtained from a co-continuous blend of two biodegradable polymers. Biomaterials 25 (2004) 5965-5978. DOI: 10.1016/j.biomaterials.2004.01.065

[34] S.Y. Park, C.S. Ki, Y.H. Park, K.G. Lee, S.W. Kang, H.Y. Kweon, H.J. Kim. Functional recovery guided by an electrospun silk fibroin conduit after sciatic nerve injury in rats. J Tissue Eng Regen Med (2012). DOI: 10.1002/term.1615

[35] Y. Yang, F. Ding, J. Wu, W. Hu, W. Liu, J. Liu, X. Gu. Development and evaluation of silk fibroin-based nerve grafts used for peripheral nerve regeneration. Biomaterials 28 (2007) 5526-5535. DOI: 10.1016/j.biomaterials.2007.09.001

[36] H. Wu, J. Zhang, Y. Luo, Y. Wan, S. Sun. Mechanical properties and permeability of porous chitosan–poly(p-dioxanone)/silk fibroin conduits used for peripheral nerve repair. Journal of the Mechanical Behavior of Biomedical Materials 50 (2015) 192-205. DOI. 10.1016/j.jmbbm.2015.06.016

[37] S. Madduri, K. Feldman, T. Tervoort, M. Papaloïzos, B. Gander. Collagen nerve conduits releasing the neurotrophic factors GDNF and NGF. Journal of Controlled Release 143 (2010) 168-174. DOI: 10.1016/j.jconrel.2009.12.017

[38] K.S. Topp, B.S. Boyd. Structure and Biomechanics of Peripheral Nerves: Nerve Responses to Physical Stresses and Implications for Physical Therapist Practice. Physical Therapy 86 (2006) 92-109. DOI: 10.1093/ptj/86.1.92

[39] S. Wang, L. Cai. Polymers for Fabricating Nerve Conduits. International Journal of Polymer Science (2010). DOI: 10.1155/2010/138686

[40] Y. Wang, D.D. Rudym, A. Walsh, L. Abrahamsen, H.-J. Kim, H.S. Kim, C. Kirker-Head, D.L. Kaplan. In vivo degradation of three-dimensional silk fibroin scaffolds. Biomaterials 29 (2008) 3415-3428. DOI: 10.1016/j.biomaterials.2008.05.002

[41] Y. Yang, X. Chen, F. Ding, P. Zhang, J. Liu, X. Gu. Biocompatibility evaluation of silk fibroin with peripheral nerve tissues and cells in vitro. Biomaterials 28 (2007) 1643-1652. DOI: 10.1016/j.biomaterials.2006.12.004

[42] X. Tang, F. Ding, Y. Yang, N. Hu, H. Wu, X. Gu. Evaluation on in vitro biocompatibility of silk fibroin-based biomaterials with primarily cultured hippocampal neurons. Biomed Mater Res 91A (2009) 166-174. DOI: 10.1002/jbm.a.32212

[43] A. Hu, B. Zuo, F. Zhang, Q. Lan, H. Zhang. In Vitro Evaluation of the Growth and Migration of Schwann Cells on Electrospun Silk Fibroin nanofibers. Advanced Materials Research 175-176 (2011) 220-223. DOI: 10.4028/www.scientific.net/AMR.175-176.220

[44] Q. Zhang, Y. Zhao, S. Yan, Y. Yang, H. Zhao, M. Li, S. Lu, D.L. Kaplan. Preparation of uniaxial multichannel silk fibroin scaffolds for guiding primary neurons. Acta Biomaterialia 8 (2012) 2628-2638. DOI: 10.1016/j.actbio.2012.03.033

[45] A. Sagnella, A. Pistone, S. Bonetti, A. Donnadio, E. Saracino, M. Nocchetti, C. Dionigi, G. Ruani, M. Muccini, T. Posati, V. Benfenati, R. Zamboni. Effect of different fabrication methods on the chemo-physical properties of silk fibroin films and on their interaction with neural cells. RSC Adv. 6 (2016) 9304-9314. DOI: 10.1039/C5RA20684G

[46] F. Zhang, R. Liu, B.Q. Zuo, J.Z. Qin. Electrospun silk fibroin nanofiber tubes for peripheral nerve regeneration. 4th International Conference on Bioinformatics and Biomedical Engineering (2010). DOI: 10.1109/ICBBE.2010.5514821

[47] A.M. Ghaznavi, L.E. Kokai, M.L. Lovett, D.L. Kaplan, K.G. Marra. Silk Fibroin Conduits. A Cellular and Functional Assessment of Peripheral Nerve Repair. Ann Plast Surg 66 (2011) 273-279. DOI: 10.1097/SAP.0b013e3181e6cff7

[48] G. Ronchi, M: Morano, F. Fregnan, P. Pugliese, A. Crosio, P. Tos, S. Geuna, K. Haastert-Talini, G. Gambarotta. The Median Nerve Injury Model in Pre-clinical Research - A Critical Review on Benefits and Limitations. Front. Cell. Neurosci. 13 (2019) 288. DOI: 10.3389/fncel.2019.00288

FIGURES

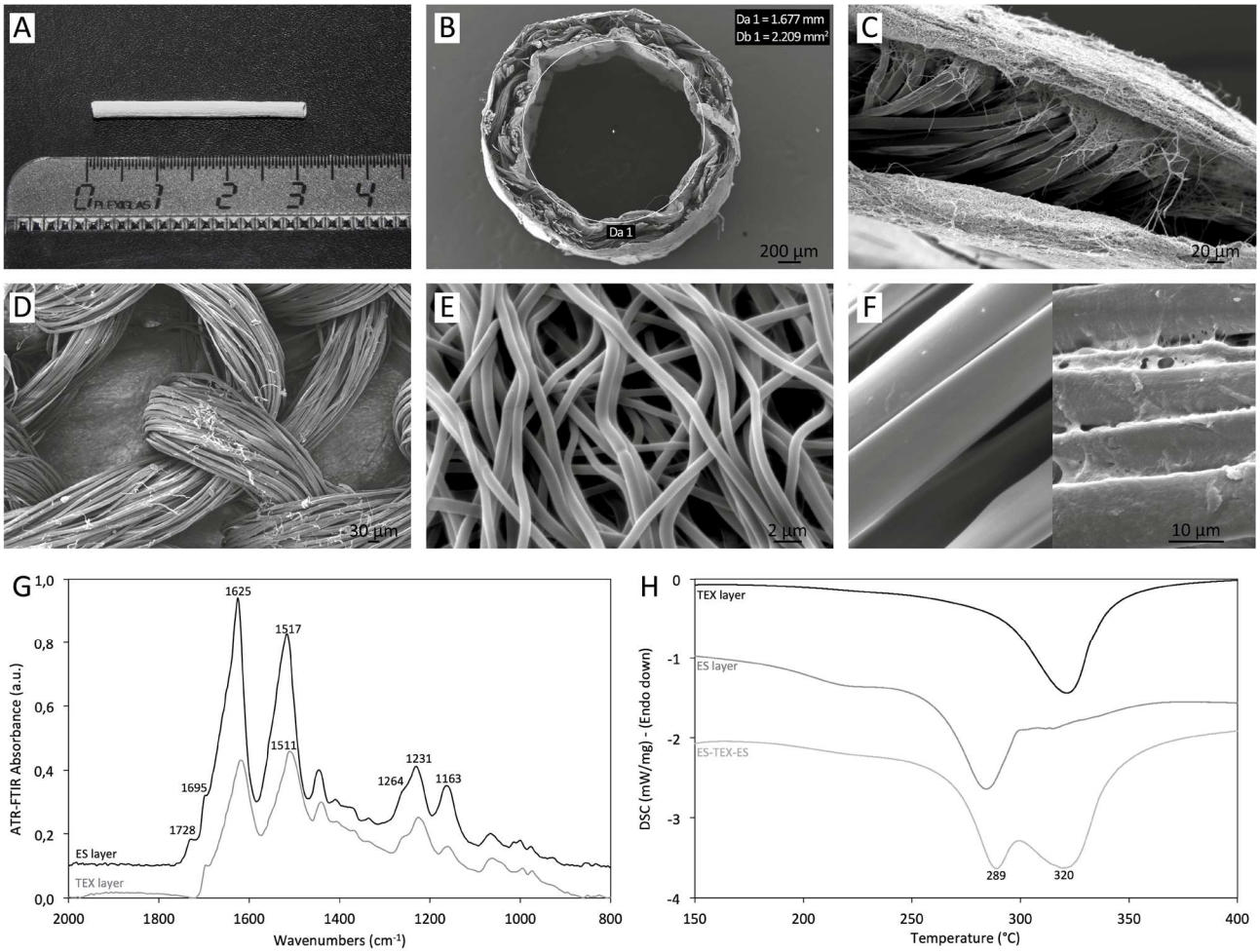

Figure 1.

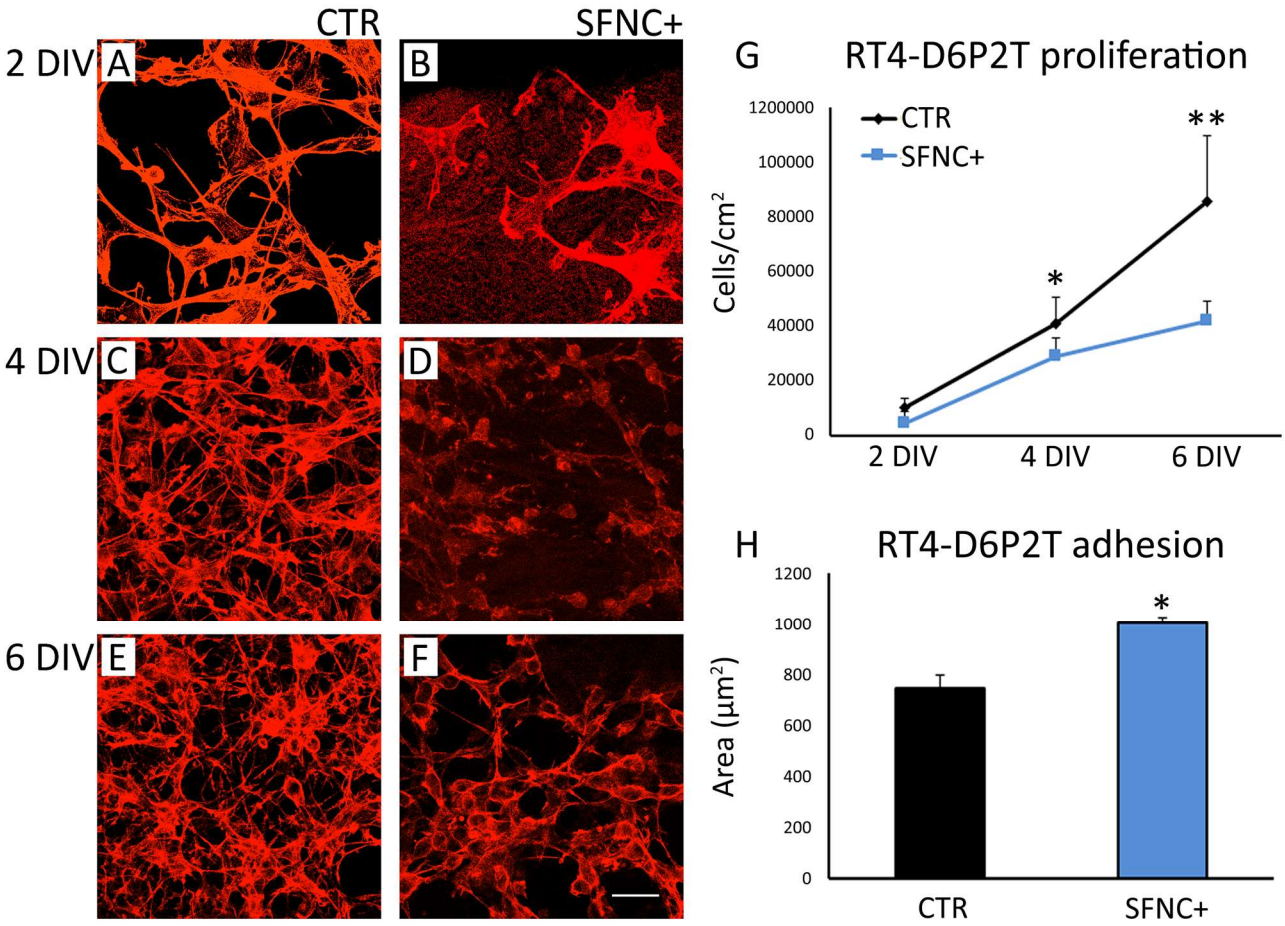
CTR
SFNC+
2 DIV
A
B
4 DIV
C
D
6 DIV
E
F
G
RT4-D6P2T proliferation
CTR
SFNC+
Cells/cm²
1200000
100000
80000
60000
40000
20000
0
2 DIV
4 DIV
6 DIV
*
**
H
RT4-D6P2T adhesion
Area (µm²)
1200
1000
800
600
400
200
0
CTR
SFNC+
*

Figure 2.

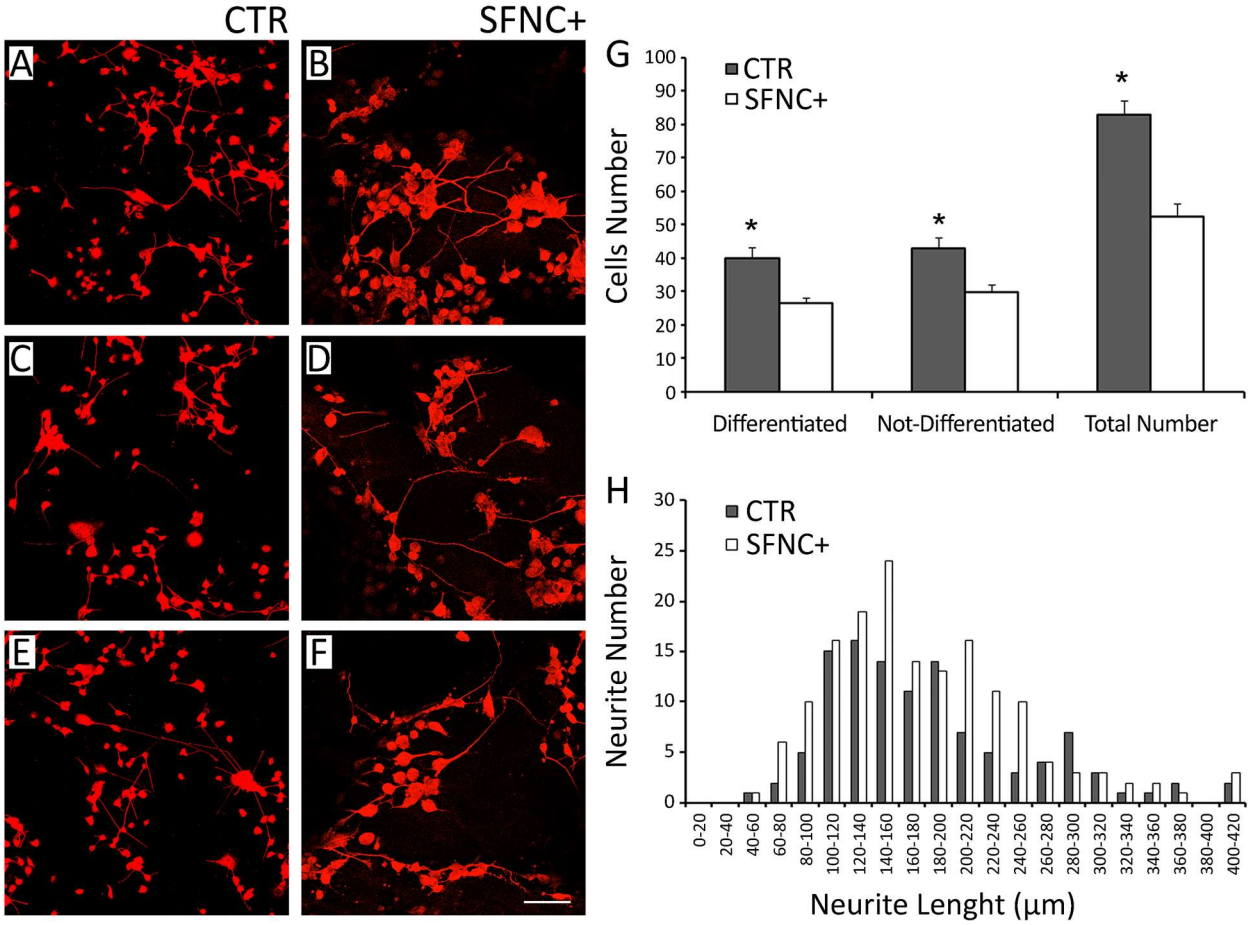
CTR
SFNC+
A
B
C
D
E
F
G
CTR
SFNC+
Cells Number
100
90
80
70
60
50
40
30
20
10
0
*
*
*
Differentiated
Not-Differentiated
Total Number
H
CTR
SFNC+
Neurite Number
30
25
20
15
10
5
0
0-20
20-40
40-60
60-80
80-100
100-120
120-140
140-160
160-180
180-200
200-220
220-240
240-260
260-280
280-300
300-320
320-340
340-360
360-380
380-400
400-420
Neurite Lenght (µm)

Figure 3.

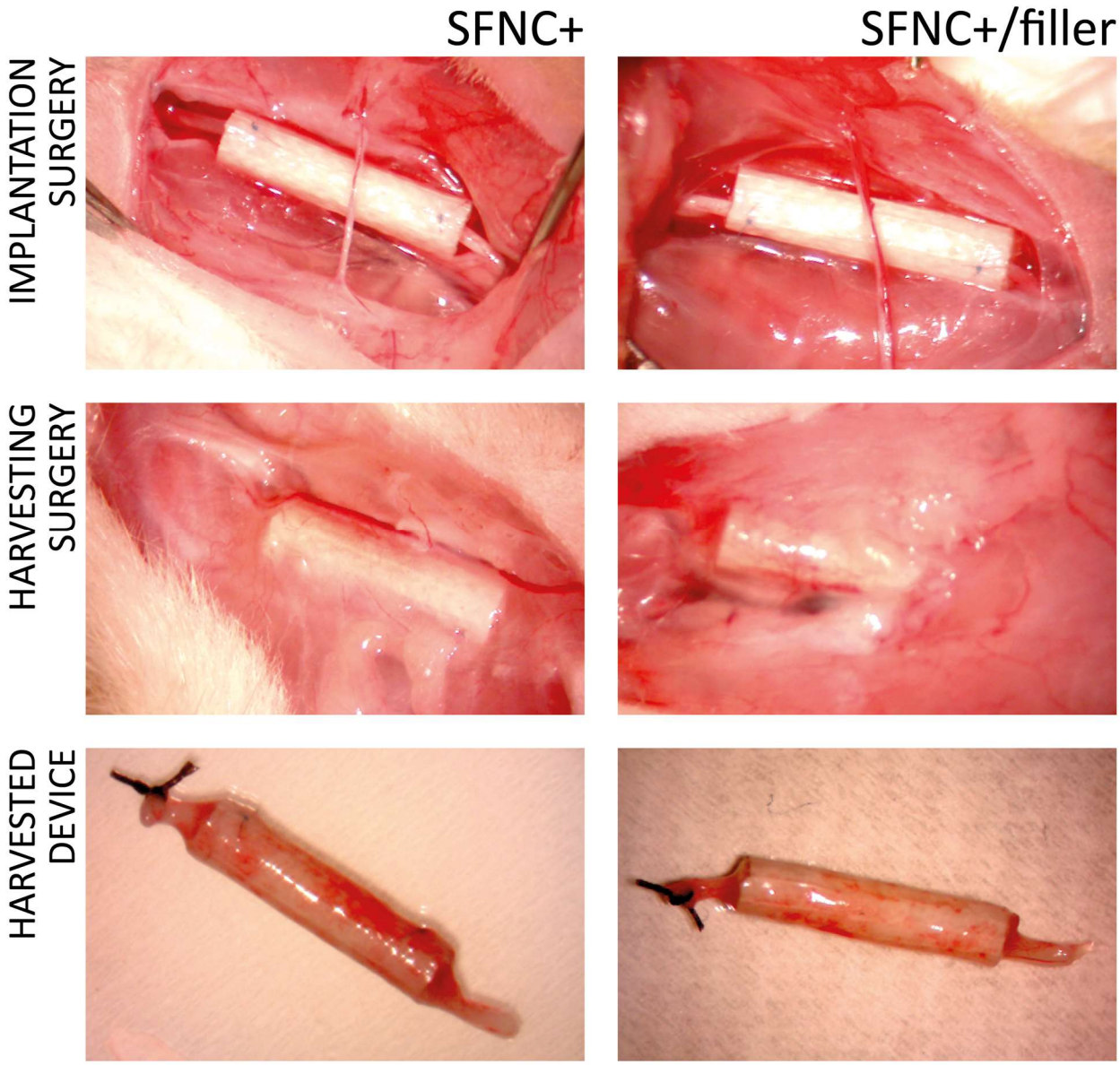
SFNC+
SFNC+/filler
IMPLANTATION SURGERY
HARVESTING SURGERY
HARVESTED DEVICE

Figure 4

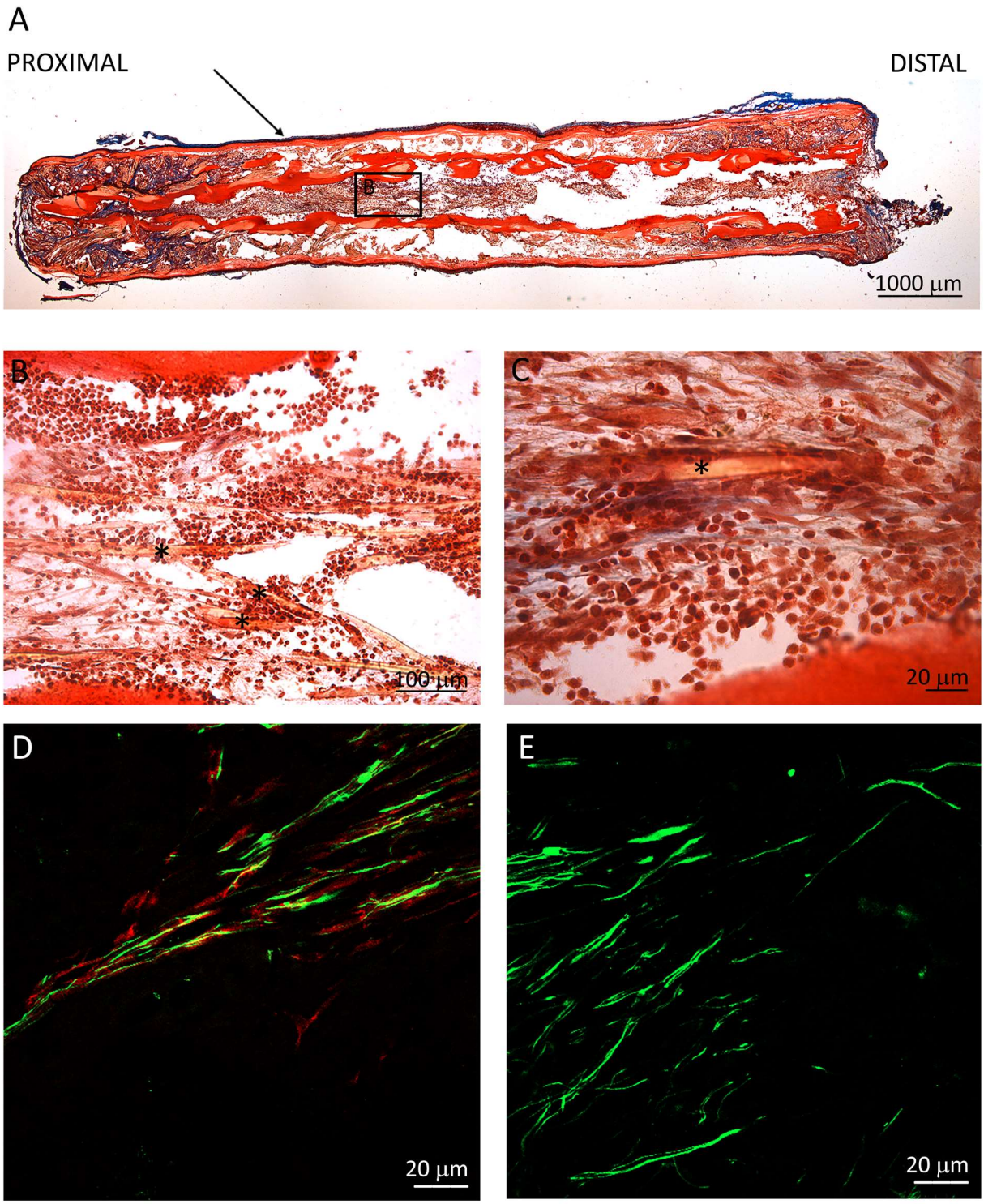

Figure 5.

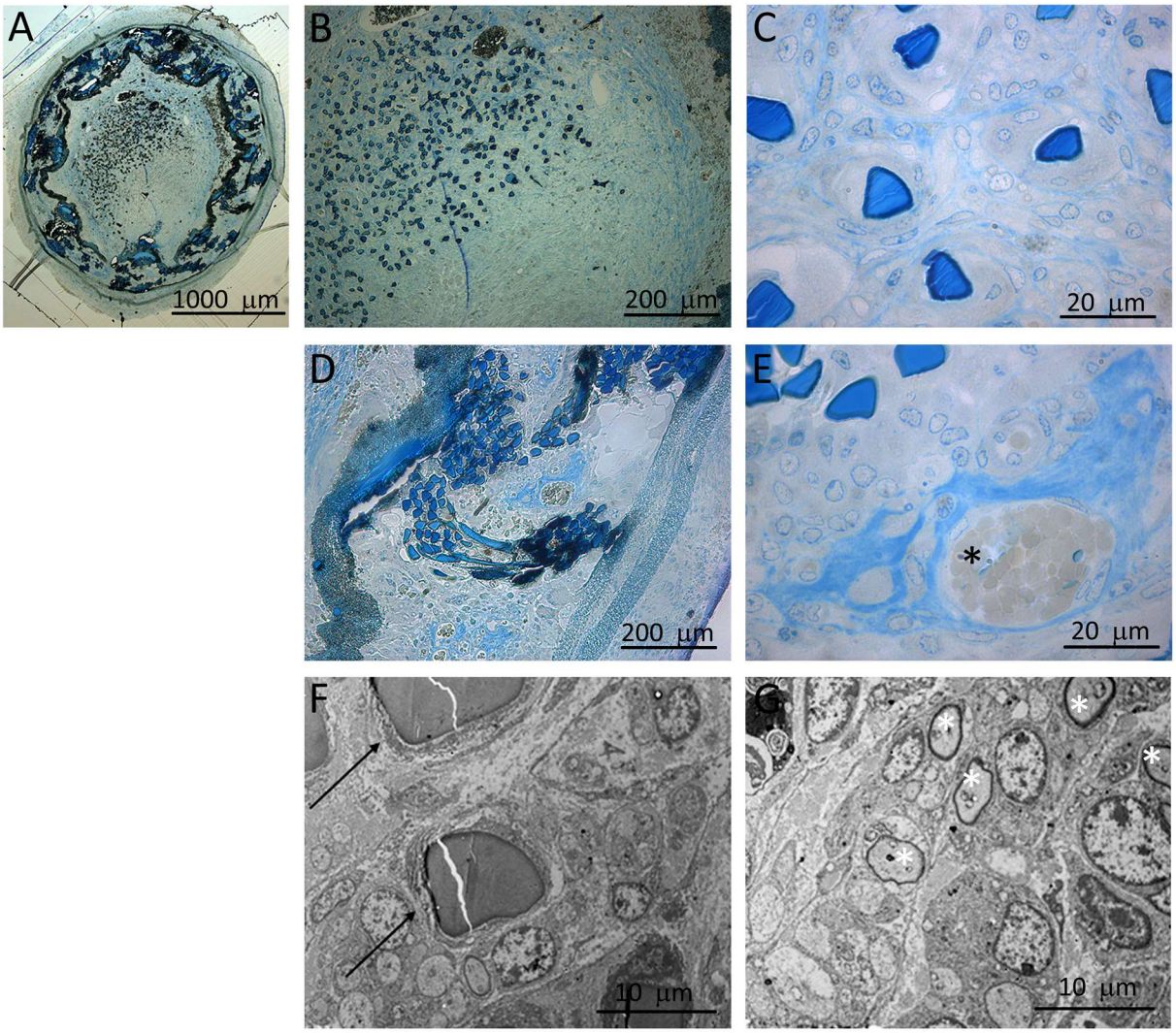

Figure 6.

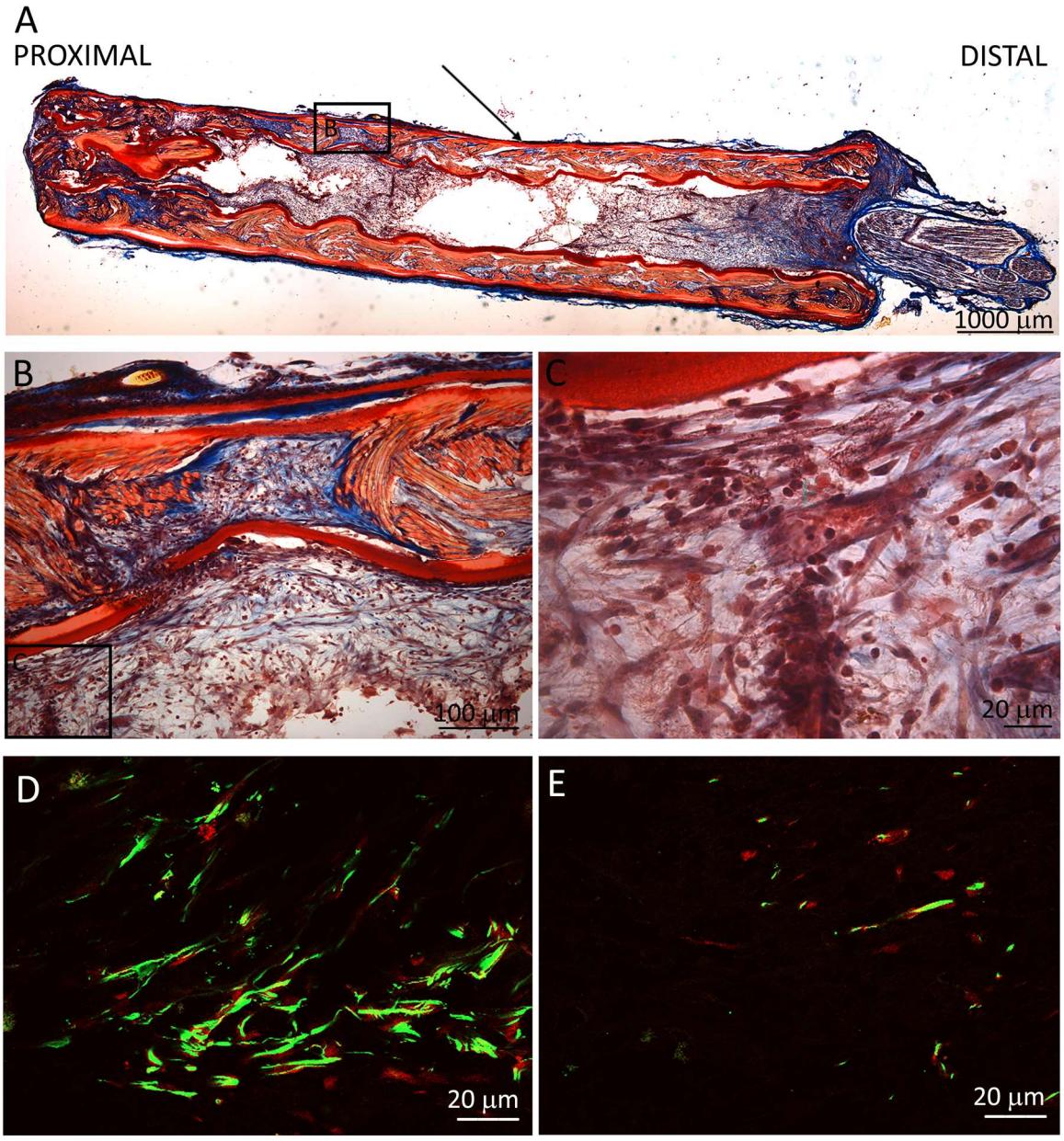

Figure 7.

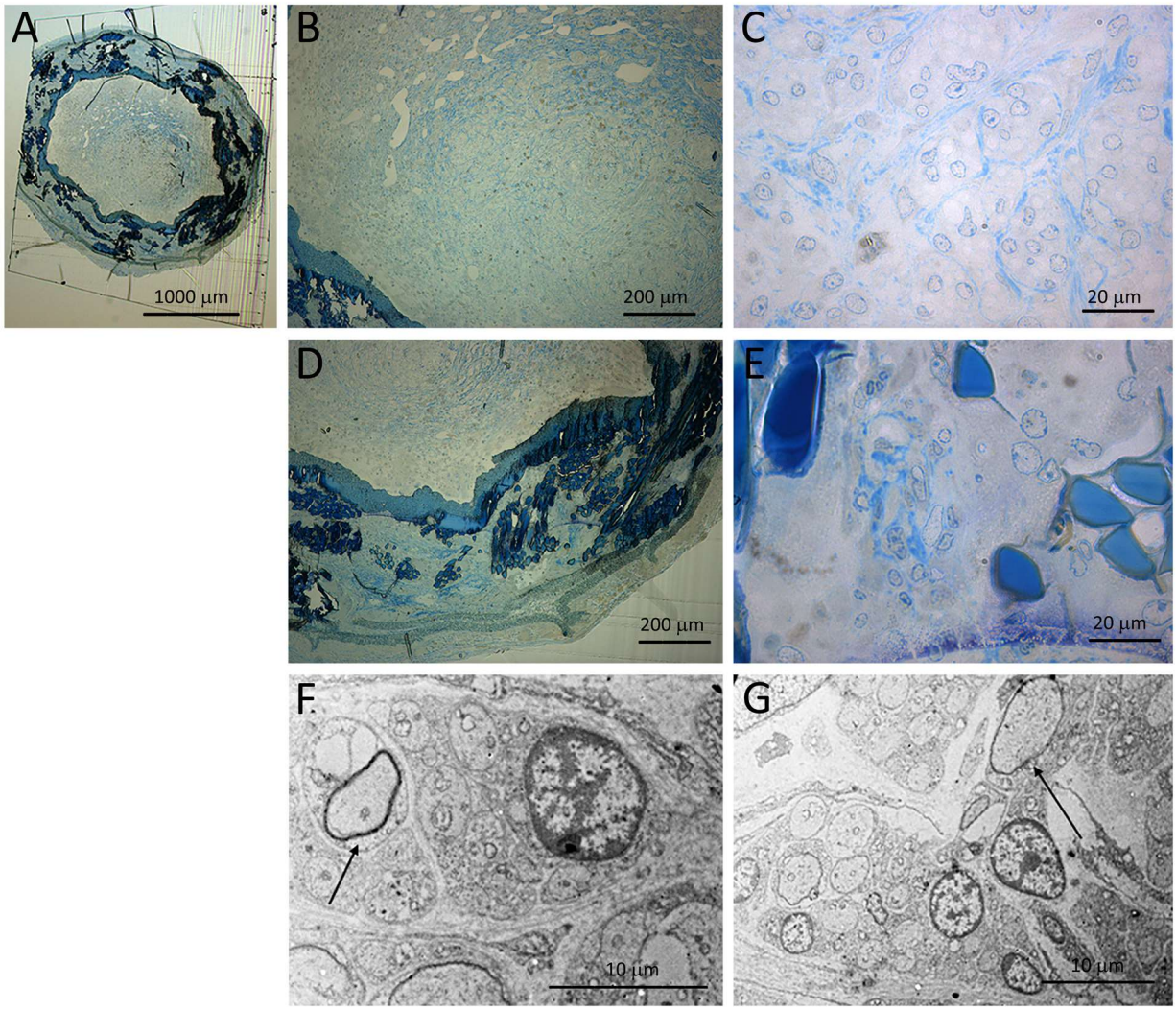

Figure 8.

FIGURE CAPTIONS

Figure 1. Morphological and physical properties of SilkBridge™. (A) "*SFNG+*" conduit design; length: 3 cm; nominal inner diameter: 1.5 mm. (B) SEM cross-section of the graft of panel A showing the two inner and outer ES layers that enclose the intermediate TEX layer (Mag 90x). (C) Detail of panel B showing a magnification of the wall structure (Mag 600x). (D) Detail of the TEX layer, in the form of braided mesh, coupled to an ES layer, visible in the background (Mag 150x). (E) SEM picture of SF nanofibers of the ES layer (Mag 10000x). (F) SEM picture of SF microfibers of the TEX layer. Left panel: "*SFNG*" design; right panel: "*SFNG+*" design, with the SF film coating the microfiber surface (Mag 4000x). (G) ATR-FTIR spectra of TEX and ES layers in the 2000-800 cm^{-1} range. (H) DSC thermograms of TEX layer, ES layer, and finished SilkBridge™ device in the 150-400°C temperature range.

Figure 2. Cell direct contact assay with SilkBridge™ conduit ("SFNC+" design): RT4-D6P2T cell line. (A-F) Representative images depicting RT4-D6P2T cells cultivated on the control substrate (A-C-E) and on SF conduit (B-D-F), stained with phalloidin. Scale bar: 20 μm. (G) Proliferation curve experiment. RT4-D6P2T cell line were cultivated on the control substrate and on the inner part of the SF conduit (cut lengthwise). Results showed a significant lower proliferation for cell line cultured on SF, but a significant higher cell dimension, indicating an involvement of the biomaterial in promoting the organization of cell architecture (H). *: $p < 0.05$, **: $p \leq 0.01$.

Figure 3. Cell direct contact assay with SilkBridge™ conduit ("SFNC+" design): NSC-34 cell line. (A-F) NSC-34 cell line was tested on SF conduits and compared with the same cells grown and differentiated on a substrate of control. Representative images depicting NSC-34 cultivated on the control (A-B-C) and SF conduit (D-E-F), stained with β-tubulin antibody. (G) Bar graph depicting the number of differentiated and not-differentiated neurons cultured on CTR and SF conduit. (H) Bar graph showing the evaluation of the neurite extension from the differentiated NSC-34 cells on CTR and SF substrates. *: $p < 0.05$, **: $p \leq 0.01$. Scale bar: 100 μm.

Figure 4. Macroscopical evaluation of SilkBridge™ conduit ("SFNC+/filler" and "SFNC+" design). IMPLANTATION: SilkBridge™ conduits were used to repair a 10 mm long median nerve gap. REMOVAL (2 weeks after surgery): SilkBridge™ conduit implantation site exposed before the harvesting (upper part); SilkBridge™ conduits detached from the surrounding tissue (lower part).

Figure 5. Median nerve repaired with SilkBridge™ conduit ("SFNC+/filler" design) at 2 weeks: light and confocal microscopy analysis. Representative longitudinal reconstruction of median nerve repaired with SF conduit filled with silk fibroin fibers 2 weeks after surgery analyzed by Masson's

trichrome staining. (A) Thin layer of connective tissue (blue, black arrow) outside the SF conduit. (B-C) Microphotographs showing the interaction between SF conduit and regenerating cellular populations (asterisks). (D-E) Microphotographs showing the presence of many regenerating neurofilament (green) positive fibers at the proximal portion of the SF conduit associated with glial cells (red).

Figure 6. Median nerve repaired with SilkBridge™ conduit ("SFNC+/filler" design) at 2 weeks: high resolution light microscopy and ultrastructural analysis. (A) Representative high-resolution light micrographs of toluidine blue-stained semi-thin proximal cross-sections. (B-C) Images taken inside the conduit. (D-E) Images taken at the conduit wall. (F-G) Representative electron microscopy images of regenerated median nerve repaired with SF conduit filled with fibroin fibers. Images were taken inside the grafts, proximally, at different magnifications. Black arrows mark native SF microfibers and their interaction with cells; asterisks mark regenerated myelinated fibers.

Figure 7. Median nerve repaired with SilkBridge™ conduit ("SFNC+" design) at 2 weeks: light and confocal microscopy analysis. Representative longitudinal reconstruction of median nerve repaired with empty SF conduit 2 weeks after surgery analyzed by Masson's trichrome staining. (A) Thin layer of connective tissue (blue, black arrow) outside the SF conduit. (B-C) Microphotograph showing the interaction between the conduit wall and regenerating cellular populations. (D-E) Microphotographs showing the presence of many regenerating neurofilament (green) positive fibers at the proximal portion of the SF conduit associated with glial cells (red).

Figure 8. Median nerve repaired with SilkBridge™ conduit ("SFNC+" design) at 2 weeks: high resolution light microscopy and ultrastructural analysis. (A) Representative high-resolution light micrographs of toluidine blue-stained semi-thin proximal cross sections. (B-C) Images taken inside the conduit. (D-E) Images taken in the conduit wall. (F-G) Representative electron microscopy images of regenerated median nerve repaired with SF conduit after 2 weeks after nerve repair. Images were taken inside the grafts, proximally, at different magnifications. Black arrows mark regenerated myelinated fibers.

TABLES

Table 1. Geometrical and mechanical properties of SilkBridge™ *.

Inner Diameter (mm)	Wall Thickness (mm)	Wall porosity (%)	Unit Weight (mg/cm)	Weight ratio (%) **	
				ES Layers	TEX Layer
1.65 ±0.07	0.52 ± 0.05	82.5 ± 1.1	7.8 ± 0.9	59 ± 3	41 ± 3

* Data refer to "*SFNC+*" design. Figures for the "*SFNC*" design are identical.

** Calculated from the intensity of the DSC endotherms.

Table 2. Values of compression strength at different strain.

	SilkBridge™ design	Compression Strength (N/m)		
		20% Strain	40% Strain	60% Strain
Dry state	"*SFNC*"	30.1 ± 0.2	91.7 ± 17.2	461.5 ± 72.6
	"*SFNC+*"	261.7 ± 75.9	341.4 ± 82.7	537.7 ± 130.8
Wet state	"*SFNC*"	5.9 ± 0.7	14.9 ± 1.5	95.5 ± 7.4
	"*SFNC+*"	15.1 ± 1.9	37.1 ± 3.2	192.2 ±.27.2
	"*SFNC+/filler*"	11.6 ± 3.0	50.1 ± 13.4	843.4 ± 196.4

SUPPLEMENTARY MATERIALS

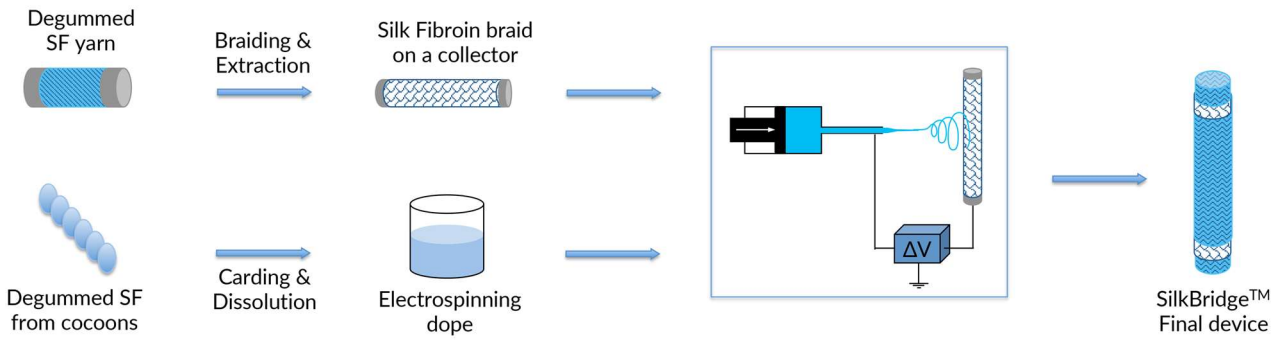

Scheme S1. Manufacturing flowchart of SilkBridge™.

SilkBridge™ is made from two different sources of silk fibroin: degummed silk yarn (top line, left) and silk cocoons (bottom line, left). Both yarn and cocoons are acquired from external suppliers and checked internally for quality. The degummed silk yarn is braided in tubular shape by needle braiding and then purified by methanol Soxhlet extraction (TEX layer). Cocoons are degummed to remove sericin. The pure silk fibroin thus obtained is dissolved in Lithium Bromide 9.3 M and dialyzed against distilled water. The aqueous silk fibroin solution is cast to obtain pure silk fibroin films, which are dissolved in formic acid for the preparation of the electrospinning dope (silk fibroin concentration: 8% w/v). Inner and outer ES layers of the tubular device are built onto the two surfaces of the TEX layer assembled on a mandrel. Before electrospinning, each surface of the TEX layer is coated with a solution of ionic liquid (1-ethyl-3-methylimidazolium acetate; EMIMAc) in distilled water (80:20 v/v). Procedural details of this manufacturing step are still under patenting and cannot be fully disclosed. After the deposition of each ES layer, the tubular structure is consolidated with aqueous ethanol (80% vol), washed with water overnight, dried and checked for quality. The final three-layered ES-TEX-ES tubular scaffold is finally purified with ethanol by microwave assisted extraction, packaged in double pouches under laminar flow cabinet and sterilized with ethylene oxide (EtO).

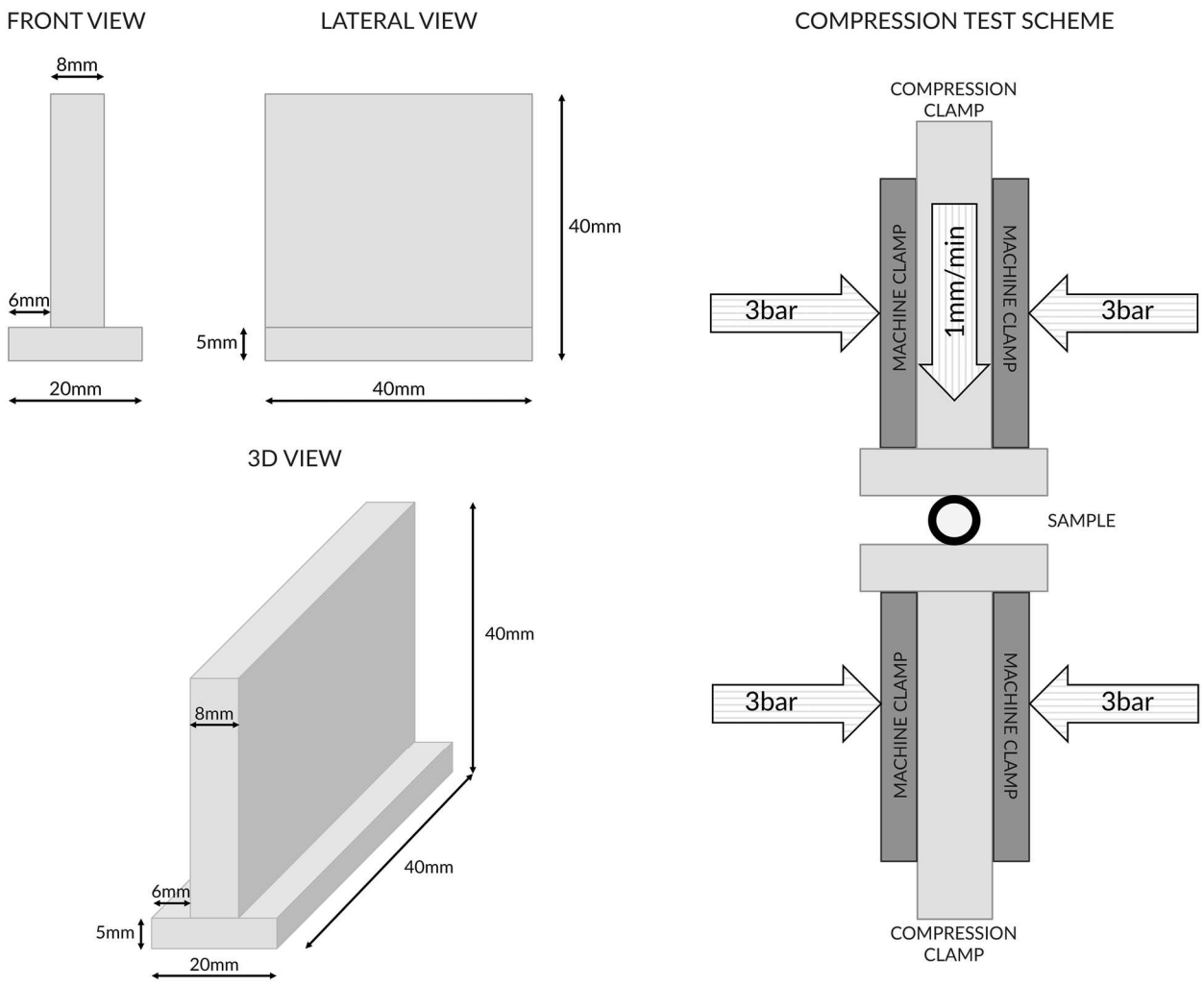

Scheme S2. Technical details of the grips used for compression tests.

Technical drawing showing the dimensions of the Aluminum-made T-shaped device designed and used for the compression tests (left). The T-shaped devices are clamped in the upper and lower tensile machine grips (right). The sample under testing is placed onto the surface of the lower grip, and then the upper grip is moved down until it comes into close contact with the sample. Then, grips with sample inside are fully immersed in the thermostatic water bath at 37°C and the compression cycle is started after a conditioning period of 5 min.

Table of Content Entry

SilkBridge™: off-the-shelf nerve conduit with a novel hybrid textile-electrospun tubular architecture, highly biocompatible, and effective to sustain *in vivo* regeneration of nerve fibers.